Search for New Physics in the Same Sign Dilepton final state with b Jets and Missing Energy at the LHC

D. Barge, C. Campagnari, D. Kovalskyi, V. Krutelyov

University of California, Santa Barbara

W. Andrews, G. Cerati, D. Evans, F. Golf, I. MacNeill, S. Padhi, Y. Tu, F. Würthwein, A. Yagil, J. Yoo

University of California, San Diego

L. Bauerdick, K. Burkett, I. Fisk, Y. Gao, O. Gutsche, B. Hooberman, S. Jindariani, J. Linacre, V. Martinez Outschoorn

Fermi National Accelerator Laboratory, Batavia, Illinois

Abstract

A search for New Physics in the same sign dilepton final state with at least two b jets and $\not\!\!E_T$ is performed. This analysis uses a data sample collected with the CMS detector of pp collisions at a centre-of-mass energy of 7 TeV, corresponding to an integrated luminosity of $4.68\ \mathrm{fb}^{-1}$. For these searches, the dominant background is from $t\bar{t}$ events. No excess above the standard model background expectation is observed. Upper limits at 95% confidence level are set on the number of observed events. These limits are used to set constraints on a number of new physics models. Information on acceptance and efficiencies are also provided so that our results can be used to confront additional models in an approximate way.

1 Introduction

The CMS Collaboration has reported results of searches in the final states with two same-sign isolated leptons, jets and missing energy [2, 3, 4], including a more specific search targeting the same-sign top pair production [1]. The major background in all these analyses is from $t\bar{t}$ production, as shown in Fig. 9.

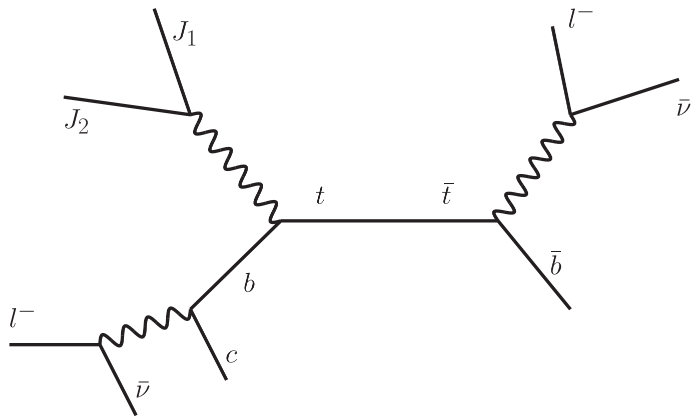

Figure 1: Diagram for $t\bar{t}$ decays giving rise to same-sign dilepton final states

The dominant source of same-sign dileptons in $t\bar{t}$ events are produced via, $t \rightarrow Wb$; where one of the leptons is from $W \rightarrow \ell\nu$ and the other originates from semi-leptonic b decays. We refer to the first as "real lepton" and the second as "fake lepton". An additional requirement on the number of b jets ≥ 2, reduces this background significantly, as a b-quark can not produce an isolated lepton and at the same time provide a b-tag. In other words, the two b-quarks in a top event cannot give three distinct, well separated objects: two tagged jets and one isolated lepton.

Same-sign dileptons in association with two or more b-quarks appear naturally in many new physics scenarios. They have been proposed as signatures of supersymmetry (SUSY) where heavy flavor (top or bottom) jets appear naturally [16, 17, 18, 19], in particular in processes with virtual stop contributions [20, 21], those with resonant stop [22], all alternatively described with simplified models (SMS) [23]; color-octet scalar production (either as sgluons in the context of SUSY [24], or non-SUSY in the context of minimal flavor violation [25]); models of maximal flavor violation (MaxFV) [26, 27, 28]; same-sign top quark production from flavor changing neutral currents in the top sector [33]; pair production of $T_{5/3}$ [29]; and top compositeness [30, 31, 32] among others.

Among all potential new physics models we select the following to report the sensitivity of this analysis:

1. the same-sign top pair production via Z' [1, 33];
2. the same-sign top pair production in MaxFV [28];
3. $t\bar{t}t\bar{t}\widetilde{\chi}_1^0\widetilde{\chi}_1^0$ final state via (exclusive) gluino pair production with each gluino decaying a top-stop pair and the stop decaying exclusively to top and LSP, all on-shell;
4. $t\bar{t}t\bar{t}\widetilde{\chi}_1^0\widetilde{\chi}_1^0$ final state via (exclusive) gluino pair production with each gluino decaying to a $t\bar{t}$ and LSP via a virtual stop exchange; this decay mode of the gluino would dominate if all squarks were very massive with the stop being the lightest;
5. $t\bar{t}W^+W^-\chi_1^0\chi_1^0$ final state via (exclusive) sbottom pair production with each sbottom decaying to a top and the lightest chargino, which subsequently decays to a W boson and an LSP;
6. a mix of $t\bar{t}b\bar{b}W^+W^-\widetilde{\chi}_1^0\widetilde{\chi}_1^0$ and $tt\bar{b}\bar{b}W^-W^-(+c.c.)$ final states via (exclusive) gluino pair or gluino-sbottom production where each gluino decays to a sbottom and a b-quark and the sbottom subsequently decays as $\widetilde{b} \rightarrow t\widetilde{\chi}_1^- \rightarrow tW^-\widetilde{\chi}_1^0$, as in the previous case.

The considered models thus have two to four b-jets, and two to four W bosons in the final state with varying kinematics.

All of these new physics scenarios have in common that the isolated same-sign leptons are typically decay products of on-shell W's, thus allowing us to increase the minimum lepton p_T requirements in our search to 20 GeV, which reduces backgrounds even further with respect to the analysis of Ref. [2, 3, 4]. The combination of requiring at least two b jets and increasing the lepton p_T threshold to 20 GeV reduces the standard model backgrounds by roughly a factor 20 over the more generic search.

For the purpose of this note we restrict ourselves to the ee, $e\mu$, and $\mu\mu$ final states, *i.e.*, we do not consider τ's, except in the case that the τ decays leptonically.

This note is organized as follows. A brief description of the event baseline selections is given in Section 2, followed by the definitions of the signal search regions in Section 3. Estimates of efficiencies for leptons, $\not\!\!E_T$, H_T, and b-tags, components of the event selection, are given in Section 4. This can be used to provide informaton to non-CMS members to better interpret our results (the so-called "outreach program). Data - Monte Carlo scale factors and their uncertainty are described in Section 5; these scale factors are needed to set limits on various models. We then describe methods to predict background contributions in Section 6, including predictions from simulation and from data, detailed in Section 7. Results of background predictions for the defined search regions are compared with observed events in data in Section 8, supported by an exclusive (disjoint) breakdown of contributions in Appendix A. Comparisons of the predicted and observed events, together with inputs relevant to signal selection systematic uncertainties described in Section 9, are then used to interpret our findings as upper limits on production of signal events beyond the background predictions as described in Section 10. Finally, in Section 11 we validate the efficiency model.

2 Baseline Event Selection

This analysis is based on the same-sign dilepton search documented in AN-2011/468 [3] and corresponds to an integrated luminosity of $4.68\ \mathrm{fb}^{-1}$. In that study we searched for events with two isolated same-sign leptons in association with 2 additional jets and $\not\!\!E_T$. Here we re-use most of the baseline event selection as summarized below. In addition, we require at least 2 b-tagged jets using Simple Secondary Vertex High Efficiency Medium (SSVHEM) working point tagger. This tagger relies on reconstructed secondary vertices with at least two tracks and an IP significance of at least 1.74 and provides a b-jet tagging efficiency of about 60% with a 4% (15%) systematic uncertainty for jet $p_T < 240 (> 240)$ GeV and a tagging rate of light flavor jets in the 2–5% range, increasing with the jet momentum [5, 35].

We thus discuss here only differences and briefly summarize the basic kinematics and triggers. For more details, we refer to [3].

- Events have to pass one of the dilepton triggers without an HT requirement.
- There should be at least two isolated same-sign leptons (ee, $e\mu$, and $\mu\mu$) with $|\eta| < 2.5$.
- We require both leptons to have p_T >20 GeV.
- We tighten the isolation cut on the leptons to 0.1.
- At least two particle flow jets tagged using SSVHEM tagger with $p_T > 40$ GeV and $|\eta| < 2.4$ corrected with L1FastL2L3 corrections.
- The selected jets must be separated from the leptons by $\Delta R > 0.4$ (any lepton with $p_T > 20$ GeV passing the ID and isolation selections).
- $\not\!\!E_T > 30$ GeV (we use pfMET).
- We remove dilepton events with invariant mass $M_{ll} < 8$ GeV.
- We veto events if a third lepton is satisfying the following:
  - has $p_T > 10$ GeV;
  - (an electron) passes $|\eta| < 2.5$, and a loosened identification, as the WP95 ID-only without any cut on h/e in the endcaps;
  - (for a muon) passes all identification requirements of the signal selection except for the calorimeter veto requirements;
  - has relative isolation < 0.2;
  - makes an opposite-sign same-flavor pair with either of the two "primary" leptons such that the pair has a mass within 15 GeV of the Z mass.

3 Search Regions

The count of events passing the baseline selections can be used to test the background predictions with the best available stastistical precision as this is the largest sample. We increase the sensitivity of this analysis to the models selected in Section 1 by considering events passing the following search region selections applied on top of the baseline selections.

- ++ region, including only positively charged lepton pairs for same-sign top production via Z' or in MaxFV. This selection reduces the fake-lepton and charge misidentification backgrounds, while keeping essentially all the signal, which is produced primarily from the uu initial state, due to the available PDF luminosities.
- The following tighther H_T and $\not\!\!E_T$ regions are defined to search for the SUSY production scenarios. As mentioned above, all of them have four b quarks, up to two hadronically decaying W bosons, and at least two neutrinos and two LSPs to make up for H_T and $\not\!\!E_T$, varying between the model points. A region with the best expected limit is to be used in every particular case.

    1. Low-H_T low-$\not\!\!E_T$region: $H_T > 200$ GeV, $\not\!\!E_T > 50$ GeV.
    2. Low-H_T high-$\not\!\!E_T$region: $H_T > 200$ GeV, $\not\!\!E_T > 120$ GeV.
    3. High-H_T low-$\not\!\!E_T$region: $H_T > 320$ GeV, $\not\!\!E_T > 50$ GeV.
    4. High-H_T high-$\not\!\!E_T$region: $H_T > 320$ GeV, $\not\!\!E_T > 120$ GeV.

4 Selection Efficiency

We would like to quote our results as a cross section, or cross section limit, that is as model independent as possible. For this we carefully define the acceptance, and provide enough details about the selection efficiency within that acceptance that anybody can use their favorite Monte Carlo generator of new physics, define an acceptance at the hard scatter level (status = 3 in Pythia), and correctly estimate the efficiency for this new physics model to within 50% or so (the so-called "outreach" program). The same steps are done here as in the pre-tagged sample analysis [3] with appropriate modifications considering differences in selections of leptons and an addition of the b-tagged jet requirements.

The event selection efficiency is a combination of

- the lepton identification and isolation efficiency;
- the efficiency of the $\not\!\!E_T$ requirement;
- the efficiency of the H_T requirement;
- the efficiency of the b-jet tagging requirement.

We derive efficiency functions for every component using a sample of simulated events for LM6 SUSY model point.[1)] Applicable simulation-to-data corrections (scale factors) are also evaluated based on available comparisons of these effiencies in data and simulation. As described below, the description of the lepton selections does not require an additional scale factor, and the correction for b-tagged jets is small with a scale factor of 0.96.

4.1 Definition of Acceptance

Lepton acceptance is defined for both leptons with $|\eta| < 2.4$ and $p_T > 20$ GeV. The generator-level equivalent of the H_T, $H_T^{\rm gen}$, is comprised of the sum p_T of all colored particles at the hard scatter level that have $p_T > 40$ GeV and $|\eta| < 2.5$. A generator-level $\not\!\!E_T$ equivalent, $\not\!\!E_T^{\rm gen}$, is defined as the absolute value of the vector sum of the transverse momentum of all non-interacting particles, e.g. neutrinos and LSP.

4.2 Lepton Efficiencies

The electon and muon selection efficiency dependence as a function of the lepton p_T is shown in Fig. 2. It is derived using the LM6 events passing the baseline selections applied to jets and $\not\!\!E_T$. Compared to the pre-tagged sample analysis [3], we obtain a slightly lower efficiency, consistent with the tighter requirement on isolation.

[1)] The LM6 cMSSM model point is defined by the model parameters as $m_0 = 85$ GeV, $m_{1/2} = 400$ GeV, $\tan\beta = 10$, $\mu > 0$, and $A_0 = 0$ GeV.

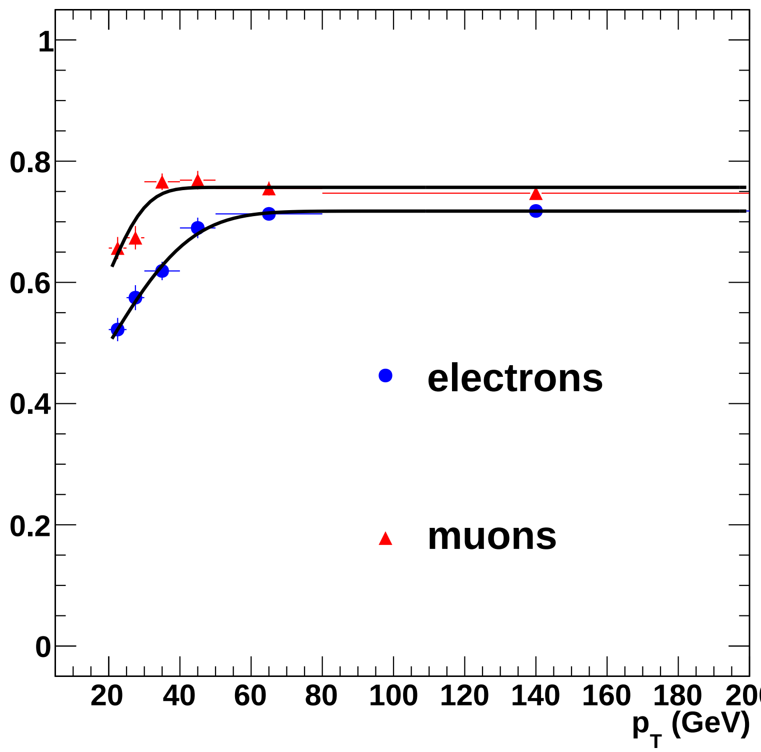

Figure 2: Lepton selection efficiency as a function of p_T, displayed for electrons and muons.

The efficiency dependence can be parameterzied as a function of p_T as

$$\epsilon = \epsilon_\infty \mathrm{erf}\left(\frac{p_T - C}{\sigma}\right) + \epsilon_C \left(1. - \mathrm{erf}\left(\frac{p_T - C}{\sigma}\right)\right), \tag{1}$$

where ϵ_∞ gives the value of the efficiency plateau at high momenta, C is equal to 20 GeV, ϵ_C gives the value of the efficiency at $p_T = C$, and σ describes how fast the transition region is. The results of the fit for electrons and muons are summarized in Table 1.

Table 1: Results of the fit of the dependence in Fig. 2 to the function specified in Eq. 1.

Parameter	Electrons	Muons
ϵ_∞	0.718 ± 0.008	0.757 ± 0.006
ϵ_C	0.498 ± 0.021	0.614 ± 0.026
σ	25.8 ± 4.0	12.9 ± 2.5

4.3 $\not\!\!E_T$ and H_T efficiency turn-on

Our selections on reconstructed jets begin with a requirement of at least two jets with $p_T > 40$ GeV. Two such jets are present in approximately 95% of the events in LM1 and LM6 with $H_T^{\mathrm{gen}} > 200$ GeV prior to any additional requirement on colored partons at the generator level beyond the sum of p_T. This represents the fraction of acceptance to two jets. In the following we proceed with determining H_T and $\not\!\!E_T$ requirement with respect to events that have generator-level requirements on the leptons and colored particles as described in Section 4.1. The efficiency for an event to pass a given reconstructed $\not\!\!E_T$ (H_T) threshold is shown in Fig. 3 as a function of $\not\!\!E_T^{\mathrm{gen}}$ (H_T^{gen}) in events passing $H_T^{\mathrm{gen}} > 200$ GeV ($\not\!\!E_T^{\mathrm{gen}} > 30$ GeV). Due to the rather small fraction of events in LM6 simulation having low H_T activity, the H_T curves are made with LM1. Results of the fits of these curves to $0.5\epsilon_\infty\{\mathrm{erf}[(x - x_{1/2})/\sigma] + 1\}$ are summarized in Table 2. Neither the $\not\!\!E_T$ nor H_T curves show a significant bias in the position of the point with half the plateau efficiency ($x_{1/2}$). The inefficiency at the plateau is essentially negligible. The width of the threshold σ increases with the value of the cut.

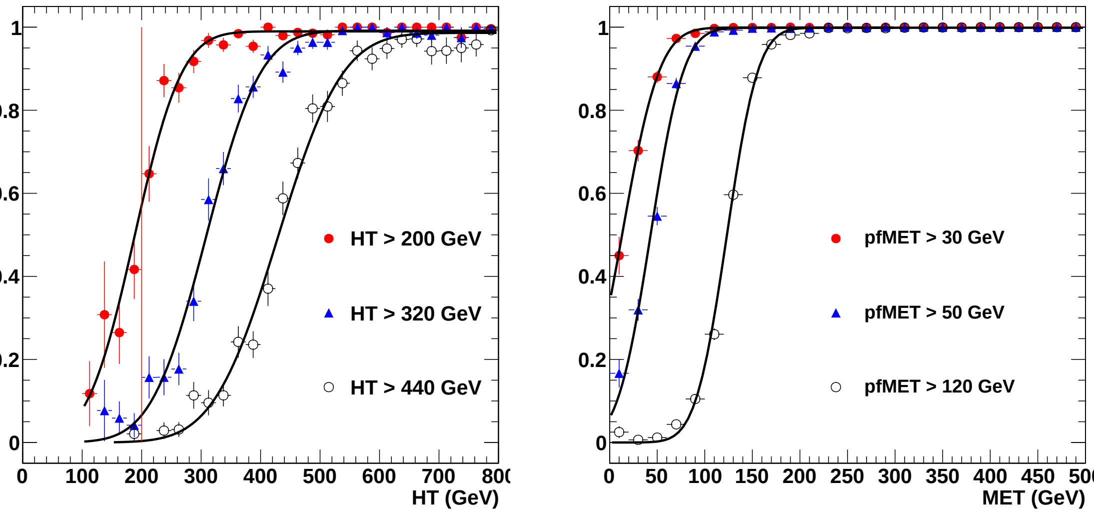

Figure 3: Efficiency for an event to pass a given reconstructed $\not\!\!E_T$ (H_T) threshold as a function of $\not\!\!E_T^{\mathrm{gen}}$ (H_T^{gen}). The curves are shown for $\not\!\!E_T$ thresholds of 30, 50, and 120 GeV; the thresholds for H_T are 200, 320, and 440 GeV.

Table 2: Results of the fit of the dependence in Fig. 3 to $0.5\epsilon_\infty\{\mathrm{erf}[(x - x_{1/2})/\sigma] + 1\}$.

Parameter	H_T			$\not\!\!E_T$		
	> 200 GeV	> 320 GeV	> 440 GeV	> 30 GeV	> 50 GeV	> 120 GeV
ϵ_∞	0.990 ± 0.002	0.992 ± 0.003	0.986 ± 0.005	0.999 ± 0.001	0.999 ± 0.001	0.999 ± 0.001
$x_{1/2}$, GeV	187.8 ± 5.5	308.4 ± 3.3	428.8 ± 3.2	13.1 ± 2.4	43.0 ± 1.1	123.3 ± 0.5
σ, GeV	88.3 ± 9.8	102.0 ± 6.2	120.3 ± 6.1	44.0 ± 2.8	38.9 ± 1.6	36.6 ± 0.9

4.4 Jet b-tagging efficiency

The b-jet tagging efficiency is defined for b-quarks passing $|\eta| < 2.5$ and matching to a reconstructed jet. A fraction of these b-quark that match to a b-tagged jet is the b-jet tagging efficiency. It shown in Fig. 4 as a function of the b-quark p_T. For b-quarks of $|\eta| < 2.5$, the b-jet tagging efficiency as a function of $p_T$can be parametrized as

- p_T< 90 GeV: $\epsilon = SF \cdot [p0 \cdot (p_t - 90\ \mathrm{GeV}) + p1]$
- 90 GeV $< p_T$< 170 GeV: $\epsilon = SF \cdot p1$
- p_T> 170 GeV: $\epsilon = SF \cdot [p2 \cdot (p_t - 170\ \mathrm{GeV}) + p1]$

where the parameters $p0$, $p1$, and $p2$ are given in Figure 4 and SF is the data-Monte Carlo scale factor: SF = 0.96 with a 4 (15)% uncertainty for jets with $p_T < 240 (> 240)$ GeV (see Section 5.2). **Make sure that the parametrization is correct.**

5 Data - Monte Carlo Scale Factors and their Uncertainties

5.1 Data - Monte Carlo Scale Factor for Leptons

The efficiencies of the lepton isolation and identification requirements (including all quality requirements) are measured with the tag&probe method in dilepton Z events using the full 2011 dataset. The efficiency of the identification requirements is a property of the lepton itself and is directly applicable to the leptons in signal events. The efficiency of the isolation requirement, however, is a strong function of all other (mainly hadronic) activity in the event. The following results are based on measurements using the full dataset and compared to simulation that is re-weighed to have a pile-up distribution comparable to that observed in data.

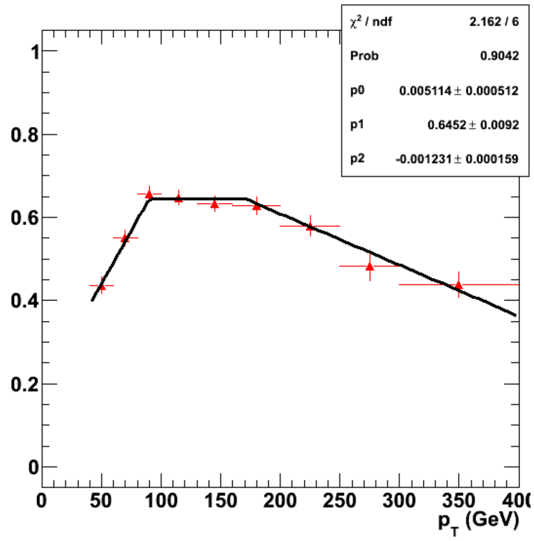

Figure 4: B-jet tagging efficiency as a function of the matching b-quark $p_T$in LM6 SUSY MC.

The electron selection efficiencies are measured in events passing the `Ele17..._SC8_Mass30` and `Ele17.._Ele8_Mass30` triggers, which require one well-identified electron and one super-cluster or GSF electron with $p_T > 8$ GeV forming a pair with a mass above 30 GeV$/c^2$. For higher p_T electrons, the `Ele32...SC_17` triggers are also used, which require one well identified electron and one super-cluster with $p_T > 17$ GeV. In the tag&probe analysis the electron tag is required to match to the well-identified electron from the trigger and also to pass all the electron requirements described in [3]. The probe electron is required to have

- $p_T > 20$ GeV, $|\eta| < 2.4$, excluding the superclusters with $1.4442 < |\eta| < 1.566$.

The isolation efficiency is measured with the probes passing all electron selections , except for the trigger requirement and the isolation itself. The identification efficiency is measured with probes passing the isolation requirement. Results of the measurement are summarized in Table 3. The contribution from the Z events is based on simple counting in the mass range of 86–96 GeV$/c$, the MC contribution includes Wjet events to match the expected residual backgrounds in this mass window. The following sources of systematic uncertainty are attributed to this measurement: background contribution, selection of dielectron events, factorization of the isolation and ID parts. The size of the background contribution can be estimated using MC alone and also tested in data with the same-sign dielectron events, which should represent the number of backgrounds reasonably well. The effect of backgrounds on the measured efficiency is established to be approximately 2% for the combined identification and isolation selection efficiency. The narrow mass window used to count electron pairs introduces a bias of about 3% to the measured efficiency by rejecting failing probes that happen to have a worse resolution or a shift in the measured momentum. This bias is expected to approximately cancel in data and simulation. We include a half of the 3% as a source of systematics. Based on simulation alone, the combined selection efficiency, measured with respect to the probe electron, differs from the product of the components by approximately 1% or less depending on the momentum range. All of these effects combined give a systematic uncertainty on the total data-to-MC scale factor in the lepton selection efficiencies of 2.5% for $p_T > 20$ GeV.

The muon selection efficiencies are measured using events passing the double-muon trigger. The tag muon is required to pass all of the muon selection requirements described in [3]. The probe muon is required to pass

- $p_T > 20$ GeV$/c$;
- $|\eta| < 2.4$;
- have both the global and the tracker muon types.

Both the isolation and the identification efficiency are measured using probes failing only the requirement in question, assuming the efficiencies factorize. Results of the muon identification and isolation efficiency measurements are presented in Table 4. As expected, the identification efficiency for muons measured in data and in MC agree

		20 - 40 GeV	40 GeV -
ISO	MC	0.9268 ± 0.0004	0.9768 ± 0.0002
	DATA	0.9247 ± 0.0003	0.9737 ± 0.0002
	DATA/MC	0.9977 ± 0.0005	0.9968 ± 0.0003
ID	MC	0.8069 ± 0.0005	0.8500 ± 0.0004
	DATA	0.8005 ± 0.0005	0.8343 ± 0.0004
	DATA/MC	0.9921 ± 0.0008	0.9815 ± 0.0006
ID X ISO	MC	0.7478 ± 0.0005	0.8303 ± 0.0004
	DATA	0.7403 ± 0.0005	0.8124 ± 0.0004
	DATA/MC	0.9899 ± 0.0010	0.9784 ± 0.0007

Table 3: Electron isolation and identification efficiencies measured with the tag&probe method. The uncertainties are statistical only.

well, while there is some discrepancy for the isolation efficiency. Similar sources of systematic uncertainty are considered here as those considered for electrons. Most of the reconstructed (probe) muons are real muons and the measurement of the identification efficiency is not affected significantly by backgrounds. With the tighter mass window used here to select events, the backgrounds are estimated to be small. This narrow mass window, however, introduces a bias of about 1.5% to the measured efficiency by rejecting failing probes that happen to have a worse resolution or a shift in the measured momentum. This bias is expected to approximately cancel in data and simulation. We include a half of the 1.5% as a source of systematics. We assign a systematic uncertainty of 1% on the identification and isolation efficiency measurement from a comparison between the simple counting of Z events and fitting the mass shape to a gaussian signal and an exponential background component. Based on studies in MC events, we find that the isolation and the identification efficiencies factorize near-perfectly and do not assign any additional systematic uncertainty. The total systematic uncertainty on the muon efficiency measurement in data, simply covering the full momentum range, is 2%.

		20 - 40 GeV	40 GeV -
ISO	MC	0.9111 ± 0.0003	0.9747 ± 0.0002
	DATA	0.8969 ± 0.0003	0.9668 ± 0.0002
	DATA/MC	0.9844 ± 0.0004	0.9919 ± 0.0002
ID	MC	0.9710 ± 0.0002	0.9612 ± 0.0002
	DATA	0.9666 ± 0.0002	0.9561 ± 0.0002
	DATA/MC	0.9955 ± 0.0003	0.9947 ± 0.0003
ID X ISO	MC	0.8847 ± 0.0003	0.9369 ± 0.0002
	DATA	0.8669 ± 0.0003	0.9244 ± 0.0002
	DATA/MC	0.9799 ± 0.0005	0.9866 ± 0.0003

Table 4: Muon isolation and identification efficiencies measured with the tag&probe method. The uncertainties are statistical only.

The tag&probe results in Tables 3 and 4 show that for leptons with $p_T > 20$ GeV used in this analysis both the ID part and the isolation parts of the lepton selection are reproduced well by simulation, already within the systematic uncertainties quoted above. Application of this measurement based on Z events to the signal events incurs an additional uncertainty due to potential mismodeling of the isolation requirement. In agreement with Ref. [3], we assign a systematic uncertainty of 5% due to modeling of the isolation efficiency for signal events. Considering the small size of the difference between data and simulation reported in Tables 3 and 4, compared to the systematic uncertainty applicable to the analysis, we approximate the scale factor to be 1.0 for both simulated signal and backgrounds and propagate the uncertainty described above to the relevant part of the analysis (signal selections) described in Section 9.

5.2 Data - Monte Carlo Scale Factor for b-jets

We apply an average scale factor of 0.96 measured using $t\bar{t}$ events for the SSVHEM tagger [34]. The uncertainty on the scale factor is 4 (15)% for jets with $p_T < 240 (> 240)$ GeV, as recommended by the b-tagging POG [35] and apply it to the analysis as described in Section 9.

6 Background Contributions

We are following the same strategy in estimating the background contributions as in the pre-tagged sample analysis [3]. Contributions with genuine same-sign isolated lepton pairs are estimated from simulation, while the contributions from leptons arising from jets (fakes) and from genuine opposite-sign pairs with a lepton charge misreconstruction (charge flips) are measured in data using control samples. The data-driven estimates are described in the next section. In addition, as a reference, we are using all relevant available simulated samples to get a feeling of the expected yields from simulation alone. As will be shown later in Section 8, contributions with genuine same-sign isolated dileptons are comparable to those estimated from events with fake leptons, while the predictions from charge flips are relatively low. These findings are in fair agreement with direct estimates from simulation.

We use MC to estimate contributions from the following SM production processes with genuine same-sign isolated dileptons:

- $qqW^{\pm}W^{\pm}, WWW, WWZ, WZZ, ZZZ, WW\gamma, t\bar{t}W, t\bar{t}Z, t\bar{t}\gamma$ and double parton $W^{\pm}W^{\pm}$ with two real leptons in the final state.
- $WZ, W\gamma^{\star}$ (0.25 GeV $< m_{\gamma^{\star}} <$ 12 GeV), and ZZ with two real leptons in the final state.
- $W\gamma$ with one real lepton and a photon conversion. This background is a priori not estimated by the fake rate method because the photon is generally isolated.

Details on the samples used and the corresponding cross sections can be found in Ref. [3]. As in the pre-tagged sample analysis, we are assigning a 50% uncertainty to the expected number of events from these samples.

7 Data Driven Background Estimation Methods

We have developed two data-driven methods to estimate the two potentially dominant backgrounds. The first method provides an estimate of the number of events with fake leptons (jets misidentified as leptons). The second method is used to estimate the number of genuine leptons reconstructed with an incorrect charge sign.

7.1 Data Driven prediction for fake lepton backgrounds

We predict the background from fake leptons using the technique previously implemented in the 2010 data analysis and documented in [6] and currently used in the pre-tagged sample analysis [3]. The idea is to count the number of events for which one lepton passes all final selections and a second lepton fails the nominal requirements but passes a looser set of requirements. We refer to the former lepton as a "numerator" lepton (n), and the latter a "non-numerator" (denominator and not numerator, or $\bar{n}$). The denominator objects are also referred to as fakeable objects (FO). The ratio of "numerator" to "denominator" objects is called a "fake rate", FR (also known as tight-to-loose ratio, TL). A fake rate function is measured in an independent data sample of multijet events. This fake rate function is measured in bins of lepton p_T and $|\eta|$, separately for electrons and muons.

The numerator selections are detailed in Section 2. The denominator selections are exactly the same as in the inclusive analysis [3]. They are listed below for completeness.

Muon denominator definition is to relax the following muon requirements from Section 2:

- χ^2/ndof of global fit < 50 (was < 10);
- transverse impact parameter with respect to the selected vertex is < 2 mm (was < 200 μm);
- Iso is set to be $Iso < 0.4$ (was < 0.1).

Electron denominator definition is to relax the following electron requirements from Section 2:

- the impact parameter cut is removed (was < 200 μm);
- Iso is set to be $Iso < 0.6$ (was < 0.10).

We thus use an extrapolation in isolation (and impact parameter) to estimate the fake lepton backgrounds in both electrons and muons. This choice of the denominator is designed to be safe determining contributions from all types of fake lepton candidates arising from jets. It has already been extensively tested in the inclusive (pre-tagged) same-sign dilepton analysis [3], where the fake-isolated leptons are expected to be dominated by heavy flavor jets, in which the lepton candidate is predominantly a real lepton from b/c-quark semileptonic decays. In this analysis, as discussed in detail below, we find that isolated lepton candidates not arising from heavy flavor decays have a much larger fraction (dominant for electrons) of all fake leptons. Closure tests performed on $t\bar{t}$ simulation (still expected to be the dominant source of fakes) confirm this choice of denominator definition works here as well.

Samples of multijet (inclusive QCD) events in data are selected among events with a single lepton trigger present. The same requirements are applied to select the multijet-dominated events as in the inclusive analysis [3].

We repeat all relevant studies performed with 2011 data, as documented in Ref. [3]. These include

- extraction of the fake rates in simulation and data;
- measurement of the fake-rate dependence on the *opposite-side* jet p_T, as a measure of the dependence on the progenitor parton momentum in data;
- closure tests on $t\bar{t}$ after the baseline and search region selections.

Results of other tests performed in Refs. [3, 6] apply here in part, with the main caveat that they are the most relevant for fakes not from the heavy flavor as well:

- closure tests in W+jets and double-fake in QCD MC samples (even though none of these are expected to contribute significantly even at the baseline selection level);
- estimates of the residual W+jet and Z contamination in the sample;
- comparison with the fake rate measured in events with enhanced heavy flavor contribution using b-tagging (the variation observed here is up to about 20% for electrons and muons in both simulation and data and are fractionally much less important here).

We arrive to essentially the same conclusions on the performance of the fake-rate method as we did in the past. In particular, we find that the method works reasonably well, still with a systematic uncertainty of about 50%. In the following we summarize the measurement of the fake rate and provide several highlights of the studies with the current dataset.

The nominal fake rates are measured requiring an "opposite side" jet with $p_T > 40$ GeV, separated by $\Delta R > 1.0$ from the FO. The electron fake rates are measured separately for triggers with an isolation requirement and for triggers without any isolation requirement on the electron. Results of the measurement are summarized in Table 5 for triggers with calorimeter isolation (as used for $e\mu$ events), and in Table 6 for triggers with both the calorimeter and tracker isolation requirements (as used for ee events). Results for electron triggers without an isolation requirement are provided in Table 7 as a reference. The muon fake rates are measured using all single-muon triggers described in Ref. [3]. The measurement is summarized in Table 8.

$\lvert\eta\rvert$ \ p_T	10.000 – 15.000	15.000 – 20.000	20.000 – 25.000	25.000 – 35.000	35.000 – 55.000
0.000 – 1.000	0.2773 ± 0.0072	0.1784 ± 0.0072	0.1759 ± 0.0079	0.1789 ± 0.0084	0.2583 ± 0.0148
1.000 – 1.479	0.2749 ± 0.0121	0.2177 ± 0.0132	0.1977 ± 0.0115	0.1924 ± 0.0117	0.3026 ± 0.0197
1.479 – 2.000	0.2415 ± 0.0152	0.1806 ± 0.0137	0.1871 ± 0.0099	0.1916 ± 0.0095	0.2379 ± 0.0135
2.000 – 2.500	0.2827 ± 0.0146	0.2607 ± 0.0156	0.2420 ± 0.0119	0.2561 ± 0.0116	0.3225 ± 0.0154

Table 5: Electron fake rate measured in bins of the electron candidate p_T and η for electrons collected using triggers with a calorimeter isolation requirement.

Figures 5 and 6 show the projection on p_T and $|\eta|$ of these fake rates for electrons and muons, respectively. Electron fake rates measured for triggers with an isolation requirement are slightly higher than those for triggers without an isolation requirement, as expected. The difference, even though it's not very large, is significant enough and we treat fake rates for these triggers separately. The dependence of the fake rates on the away-jet momentum is also shown on these figures.

$\lvert\eta\rvert$ \ p_T	10.000 – 15.000	15.000 – 20.000	20.000 – 25.000	25.000 – 35.000	35.000 – 55.000
0.000 – 1.000	0.3783 ± 0.0218	0.2932 ± 0.0279	0.2365 ± 0.0298	0.2713 ± 0.0324	0.3690 ± 0.0527
1.000 – 1.479	0.3556 ± 0.0357	0.3617 ± 0.0496	0.2364 ± 0.0405	0.2353 ± 0.0460	0.4667 ± 0.0644
1.479 – 2.000	0.2326 ± 0.0372	0.1638 ± 0.0344	0.2000 ± 0.0332	0.2260 ± 0.0314	0.2793 ± 0.0426
2.000 – 2.500	0.3357 ± 0.0399	0.2736 ± 0.0433	0.2362 ± 0.0377	0.2681 ± 0.0377	0.3645 ± 0.0465

Table 6: Electron fake rate measured in bins of the electron candidate p_T and η for electrons collected using triggers with calorimeter and tracker isolation requirements.

$\lvert\eta\rvert$ \ p_T	10.000 – 15.000	15.000 – 20.000	20.000 – 25.000	25.000 – 35.000	35.000 – 55.000
0.000 – 1.000	0.1985 ± 0.0141	0.1535 ± 0.0177	0.1260 ± 0.0212	0.1567 ± 0.0247	0.2198 ± 0.0434
1.000 – 1.479	0.1951 ± 0.0253	0.1867 ± 0.0318	0.1870 ± 0.0352	0.1800 ± 0.0384	0.3333 ± 0.0624
1.479 – 2.000	0.1880 ± 0.0339	0.1696 ± 0.0355	0.1481 ± 0.0279	0.1548 ± 0.0279	0.2596 ± 0.0430
2.000 – 2.500	0.2583 ± 0.0356	0.3084 ± 0.0446	0.1797 ± 0.0339	0.2836 ± 0.0389	0.3191 ± 0.0481

Table 7: Electron fake rate measured in bins of the electron candidate p_T and η for electrons collected using triggers without isolation requirements.

$\lvert\eta\rvert$ \ p_T	5.000 – 10.000	10.000 – 15.000	15.000 – 20.000	20.000 – 25.000	25.000 – 35.000
0.000 – 1.000	0.2760 ± 0.0028	0.2127 ± 0.0024	0.1808 ± 0.0032	0.1541 ± 0.0043	0.1441 ± 0.0009
1.000 – 1.479	0.3119 ± 0.0042	0.2527 ± 0.0036	0.2100 ± 0.0048	0.1820 ± 0.0067	0.1770 ± 0.0015
1.479 – 2.000	0.3340 ± 0.0042	0.2694 ± 0.0037	0.2238 ± 0.0049	0.2197 ± 0.0072	0.2018 ± 0.0016
2.000 – 2.500	0.3343 ± 0.0061	0.2741 ± 0.0054	0.2174 ± 0.0071	0.2012 ± 0.0108	0.2150 ± 0.0027

Table 8: Muon fake rate measured in bins of the muon candidate p_T and η. The uncertainties are statistical only.

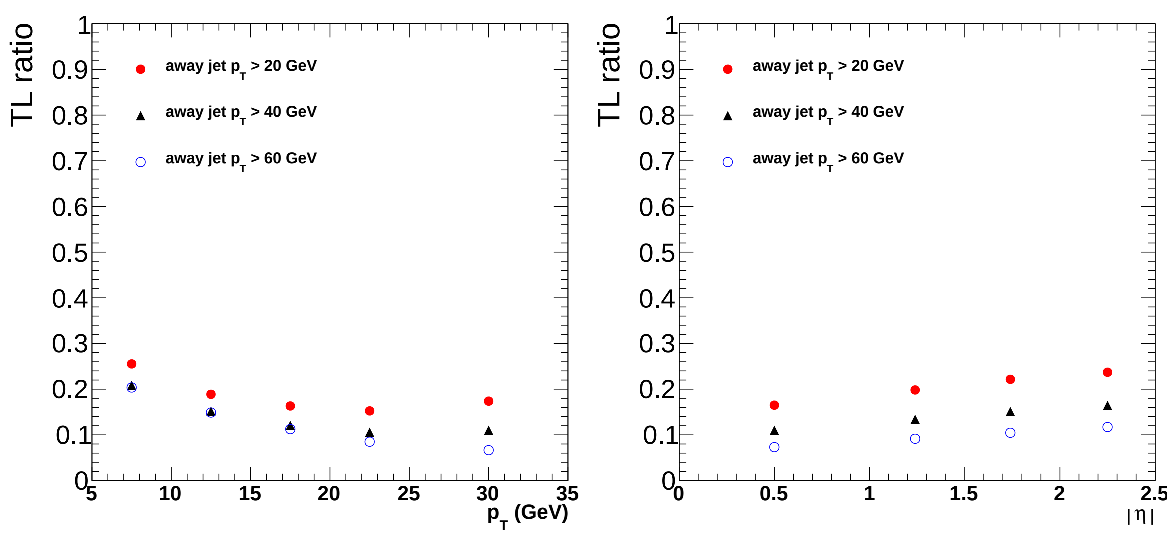

Figure 5: Muon fake rate projected on p_T (left) and $|\eta|$ (right). The fake rates are shown separately for measurements with a requirement for an away jet p_T to be above 20 GeV (red circles), 40 GeV (black circles), and 60 GeV (blue circles).

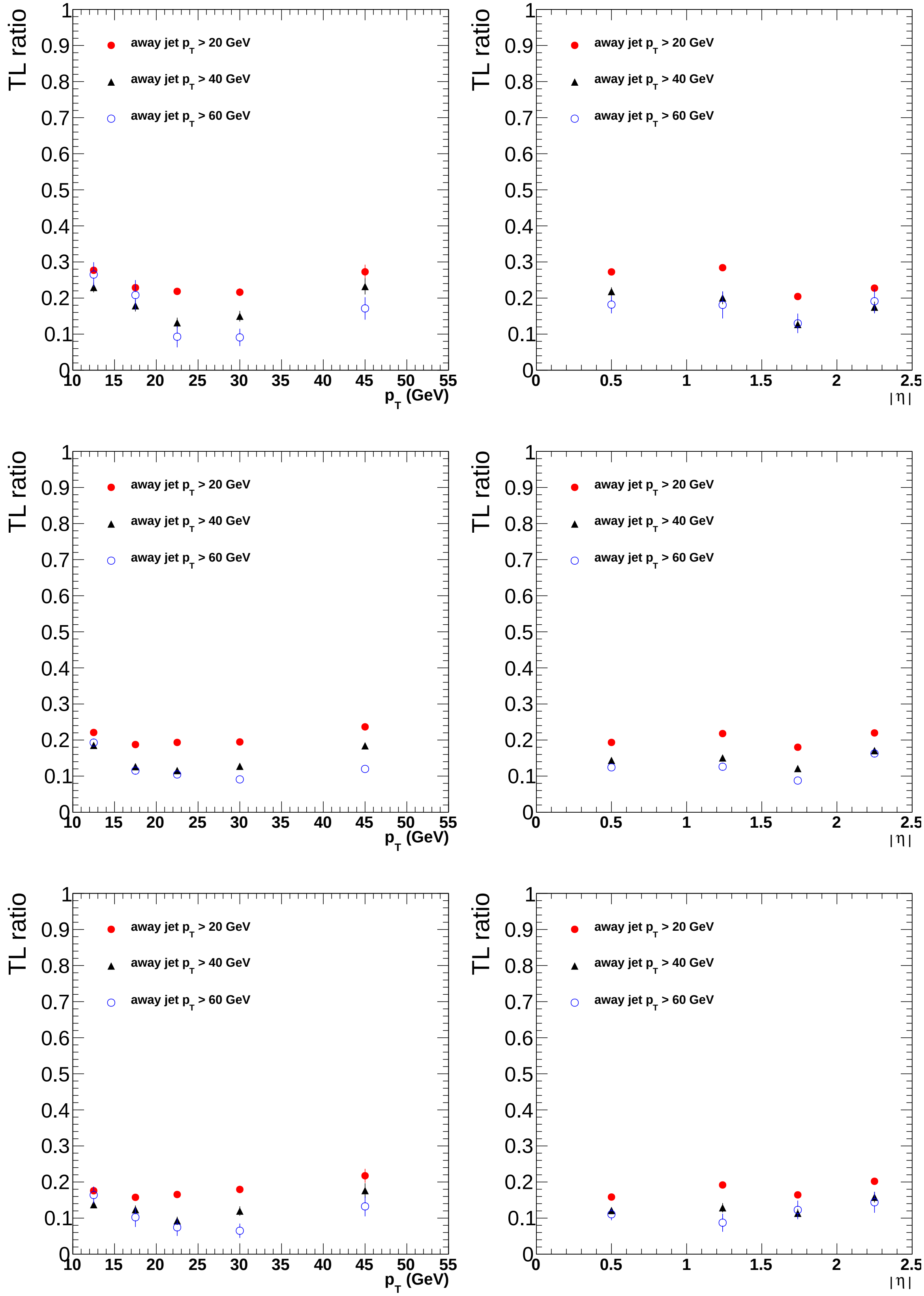

Figure 6: Electron fake rate projected on p_T (left) and $|\eta|$ (right) for electrons collected by the triggers with calorimeter and tracker isolation requirements (top), with a calorimeter isolation requirement (middle) and without an isolation requirement (bottom). The fake rates are shown separately for measurements with a requirement for an away jet p_T to be above 20 GeV (red filled circles), 40 GeV (black up triangles), and 60 GeV (blue open circles).

The application of the fake-rate method to predict this background is exactly the same as in the inclusive analysis [3]. As in the inclusive same-sign analysis, the measured fake rates are restricted to $p_T < 55(35)$ GeV for electrons (muons), where we find negligible contamination from electroweak sources (W/Z production) to the sample used to extarct the fake rates. The values for the highest measured p_T range apply for all leptons with larger momenta. Measurements for lepton $p_T < 20$ GeV are given for completeness, they are not used in the analysis.

We test that the fake rates measured in QCD are applicable to the dilepton samples by performing closure tests on the simulated $t\bar{t}$ sample.[2] Other dilepton processes with fakes, W+jets with one fake and QCD with two fakes, are expected to contribute negligibly to the events selected in this analysis; available samples for these processes do not have events passing the baseline selections. The following selections are applied to events entering the closure tests:

1. select events passing the baseline selections;
2. require that one lepton is matched to a leptonic W decay and the other (fake) lepton is not matched to a leptonic W decay;
3. scale the number of fake leptons failing the full lepton selections and passing the FO selections by $FR/(1-FR)$ as a function of the fake lepton p_T and $|\eta|$ — this is the prediction of the number of fakes passing full lepton selections;
4. compare the predicted and observed number of fake leptons.

The prediction of the number of events with fakes, averaged among modes, gives a reasonable agreement with the observed counts within the statistical uncertainties, as summarized in Table 9. Most of the events are from fake electrons, expected to contribute about 3/4 of the total. The events with muon fakes, still expected to be dominated by heavy flavor decays, are overpredicted, consistent with observations in the pre-tagged analysis [3]. The events with electron fakes, expected to be dominated by non-heavy-flavor sources, are on average predicted fairly well, while the agreement fluctuates up/down per-mode.

Selection	result	ElectronFR		Muon FR	
		ee	$e\mu$	$\mu\mu$	$e\mu$
Baseline	observed	37	31	11	4
	predicted	52 ± 4	65 ± 4	17 ± 4	15 ± 3
	δ	0.29 ± 0.13	0.52 ± 0.09	0.35 ± 0.25	0.73 ± 0.14
	$\langle\delta\rangle$	0.42 ± 0.08		0.53 ± 0.14	
	$\langle\delta\rangle$	0.44 ± 0.07			

Table 9: Fake rate closure test on $t\bar{t}$ MC events. The difference δ is defined as $(p-o)/p$, where p and o are the predicted and observed counts, respectively. The number of events are as counted in the $t\bar{t}$ MC sample.

The systematic uncertainty of $\pm 50\%$ per fake lepton is estimated for the fake rate method. This value is dominated by the results of the closure tests. Our understanding of these results is that the main underlying cause is the dependence of the fake rate on parent parton momentum. The momentum spectrum of partons from ISR/FSR differs from that of the b-jets or light-flavor-quark jets ($W \to q\bar{q}'$) arising from the $t \to Wb$ decays. The mix of the spectra varies, but the range of the fake rate variation can be tested in data QCD events used to measure the fake rate by applying varying thresholds to the away jet, as illustrated in Figs. 5 and 6.

We compute the contributions from double-fake and single-fake events separately and assign a 50% systematic uncertainty on the combined estimate.

We have neglected any ”signal contamination”. Signal contamination enters when there is a significant source of two isolated leptons, with one or both failing the numerator cuts, but passing the denominator cuts comprising a significant fraction of the total number of $N_{n\bar{n}}$ or $N_{\overline{nn}}$ samples. Without an additional correction that can be easily applied, a contribution from events with two real same-sign dileptons failing the numerator selections will overestimate the background contribution by approximately 3% of the count of the real same-sign dileptons passing the numerator selections. Considering the size of the uncertainty on the background, this effect can be

[2] A large `/TTJets_TuneZ2_7TeV-madgraph-tauola/Fall11-PU_S6_START42_V14B-v2` sample with an equivalent luminosity of about 0.4 ab^{-1} is used for the closure test.

safely ignored in the estimates of the fake leptons until the rate of same-sign dileptons passing the full selections is at least an order of magnitude higher than that expected from fakes alone.

7.2 Data Driven prediction for charge mis-reconstruction backgrounds

Following our original studies [2] of the electron charge misreconstruction, we apply the requirement for electrons that all three charge measurements for a GSF electron agree. This dramatically reduces the rate of charge mismeasurement for electrons to the point that this background is only $\approx 10\%$ of the total. Note that, while small, this is a much larger fraction than in the untagged analysis, were "fake" lepton backgrounds are dominant [2, 3, 4]. Even though this background is small, it is not necessarily well-reproduced in simulation. We apply the data-driven method used in the previous analysis[2, 3, 4] here as well.

The following steps are done:

1. Measure the probability for an electron to have its charge misreconstructed in bins of $|\eta|$ and p_T using single electron gun Monte Carlo. This is the same probability as measured in the pre-tagged same-sign sample analysis [3].
2. Calibrate this probability using Z events in data. This step should be repeated here because of the tighter isolation requirement applied to electrons.
   (a) Use a Z sample in data to control this probability. The sample is selected from dielectron events with 76 GeV $< m_{ll} <$ 106 GeV, $\not\!\!E_T <$ 20 GeV, and transverse mass $<$ 25 GeV. Here transverse mass is calculated based on whichever lepton has higher p_T.
   (b) Apply this probability to the opposite sign events in this control sample to obtain a predicted number of same-sign Z candidates. Compare this with the actual yield of double-charged Z candidates to establish validity of the approach.
   (c) If the expected and observed yields agree reasonably well in the previous step, continue using the probability measured in the first step and include the discrepancy as a systematic uncertainty.
3. Apply this (calibrated) probability to all the electrons in opposite sign dilepton events that pass the selection. This produces the data driven charge flip prediction shown in the tables in Section 8.
4. The p_T distribution of leptons from top is slightly harder than that for leptons from Z. The calibration step above thus does not fully sample the lepton spectrum for our background sample. We assign an additional systematics of 20% to account for this effect.

In the calibration step we find 390 events with same-sign electron pairs in data in the Z control region. This needs to be compared with the sum of the expected same-sign events as estimated from opposite-sign dielectrons, 360 ± 4, plus a contribution from fakes, 11 ± 6. These comparisons are consistent within statistics and no additional data-driven correction is necessary for the simulated charge misid probabilities. The number of events expected directly from simulation is 369 ± 11, also in a good agreement with the numbers above. The same-sign dielectron mass distribution observed in data is compared to the expectation from simulation in Fig. 7. The total systematic uncertainty on the charge flip prediction is 20%, accounting for both the potential residual miscalibration (less than 5%) and the difference in the lepton spectra in Drell-Yan events and in the background $t\bar{t}$ events.

8 Event Yields and Background Estimation

In the following Tables 10 to 15 summarize the background estimates and compare them to the observed counts of events in data for the baseline and search region selections defined in Sections 2 and 3. In each table the expectations from the simulation alone are given in the upper part These overall are used to get a feeling of the expected contributions. Of these, only backgrounds with actual final state same-sign leptons are used for the final result as described in Section 6. The lower part of each table is the main result of the analysis used for comparisons with data and setting constraints on various models. These include the predictions for the fake-lepton and charge misidentification bacgrounds derived as descibed in Section 7.

To reiterate and make it absolutely clear. The total background prediction in a given signal region is the sum of three distinct components:

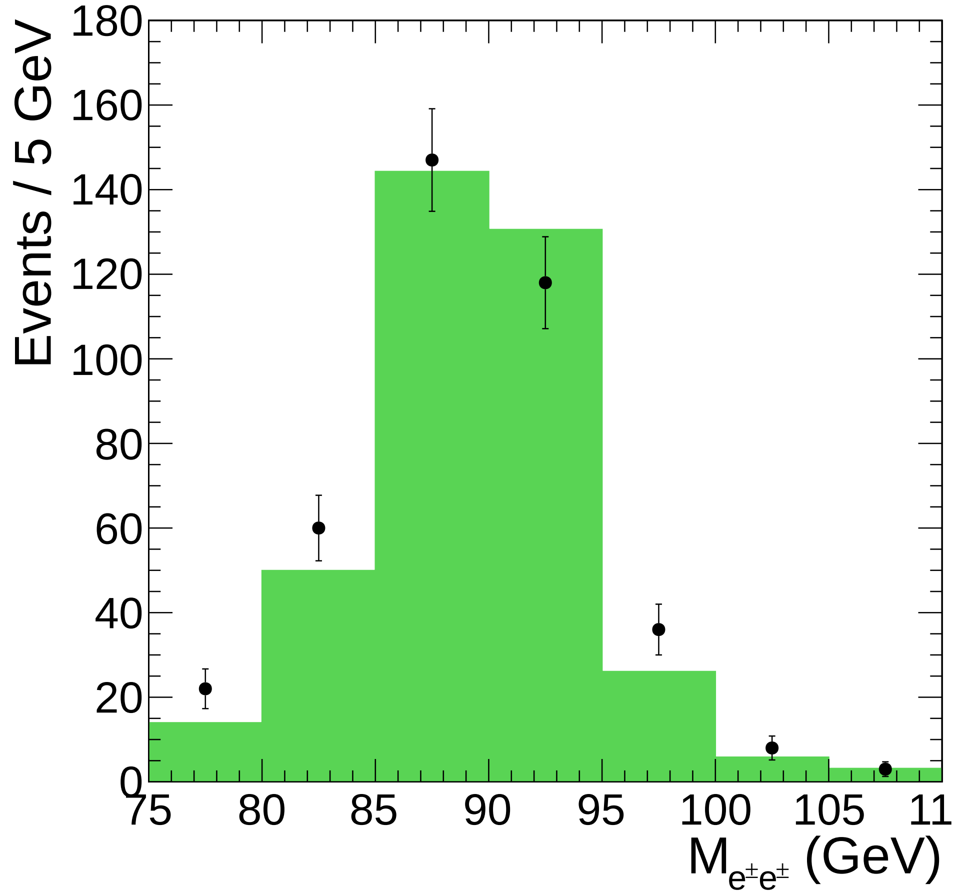

Figure 7: Same sign ee invariant mass distribution compared with $Z \to ee$ Monte Carlo expectations. Cuts on missing transverse energy $<$ 20 GeV and transverse mass $<$ 25 GeV have been applied to reduce backgrounds from $W+$ jets. The highest p_T lepton has been used in the calculation of the transverse mass.

1. The data-driven charge misid prediction (row "Charge Flips" in Tables 10 to 15).
2. The data-driven sum of single fakes (SF) and double fakes (DF) predictions (row "SF+DF" in Tables 10 to 15).
3. The total MC prediction for processes that naturally give isolated same sign dileptons, see Section 6 (row "MC Pred" in Tables 10 to 15; this is the sum of the rows starting from "$V\gamma$" down to and including the tribosons – although in practice only ttW and ttZ matter).

Details on the systematics of the background predictions are given in the corresponding sections. The final estimates on these uncertainties are rather simple:

1. The charge flip contribution has a 20% systematics.
2. The predicted number of fakes has a 50% systematics in all modes.
3. The MC prediction for "real" same sign isolated dileptons has an uncertainty of 50%.

Source	ee	$\mu\mu$	eμ	all
$t\bar{t} \to \ell\ell X$	0.604 $\pm$ 0.102	0.000 $\pm$ 0.199	0.653 $\pm$ 0.105	1.256 $\pm$ 0.147
$t\bar{t}$ other	0.000 $\pm$ 0.199	0.000 $\pm$ 0.199	0.000 $\pm$ 0.199	0.000 $\pm$ 0.199
$t\bar{t} \to \ell(b \to \ell)X$	0.069 $\pm$ 0.199	0.140 $\pm$ 0.049	0.094 $\pm$ 0.199	0.303 $\pm$ 0.074
$t\bar{t} \to \ell(\not{b} \to \ell)X$	0.546 $\pm$ 0.095	0.020 $\pm$ 0.199	0.628 $\pm$ 0.108	1.195 $\pm$ 0.145
t, s-channel	0.000 $\pm$ 0.057	0.000 $\pm$ 0.057	0.000 $\pm$ 0.057	0.000 $\pm$ 0.057
t, t-channel	0.077 $\pm$ 0.077	0.000 $\pm$ 0.055	0.000 $\pm$ 0.055	0.077 $\pm$ 0.077
tW	0.000 $\pm$ 0.045	0.000 $\pm$ 0.045	0.016 $\pm$ 0.045	0.016 $\pm$ 0.045
$Z \to ee$	0.000 $\pm$ 0.429	0.000 $\pm$ 0.429	0.000 $\pm$ 0.429	0.000 $\pm$ 0.429
$Z \to \mu\mu$	0.000 $\pm$ 0.429	0.000 $\pm$ 0.429	0.000 $\pm$ 0.429	0.000 $\pm$ 0.429
$Z \to \tau\tau$	0.000 $\pm$ 0.429	0.000 $\pm$ 0.429	0.000 $\pm$ 0.429	0.000 $\pm$ 0.429
W+jets	0.000 $\pm$ 1.808	0.000 $\pm$ 1.808	0.000 $\pm$ 1.808	0.000 $\pm$ 1.808
WW	0.000 $\pm$ 0.019	0.000 $\pm$ 0.019	0.000 $\pm$ 0.019	0.000 $\pm$ 0.019
Vγ	0.000 $\pm$ 0.248	0.000 $\pm$ 0.248	0.000 $\pm$ 0.248	0.000 $\pm$ 0.248
$W\gamma^* \to \ell\nu ee$	0.000 $\pm$ 0.097	0.000 $\pm$ 0.097	0.000 $\pm$ 0.097	0.000 $\pm$ 0.097
$W\gamma^* \to \ell\nu\mu\mu$	0.000 $\pm$ 0.075	0.000 $\pm$ 0.075	0.000 $\pm$ 0.075	0.000 $\pm$ 0.075
$W\gamma^* \to \ell\nu\tau\tau$	0.000 $\pm$ 0.028	0.000 $\pm$ 0.028	0.000 $\pm$ 0.028	0.000 $\pm$ 0.028
WZ	0.034 $\pm$ 0.012	0.017 $\pm$ 0.008	0.031 $\pm$ 0.012	0.082 $\pm$ 0.019
ZZ	0.000 $\pm$ 0.000	0.001 $\pm$ 0.001	0.002 $\pm$ 0.001	0.003 $\pm$ 0.001
dp$W^\pm W^\pm$	0.000 $\pm$ 0.004	0.000 $\pm$ 0.004	0.000 $\pm$ 0.004	0.000 $\pm$ 0.004
sp$W^- W^-$	0.000 $\pm$ 0.001	0.000 $\pm$ 0.001	0.003 $\pm$ 0.002	0.003 $\pm$ 0.002
sp$W^+ W^+$	0.000 $\pm$ 0.006	0.000 $\pm$ 0.006	0.000 $\pm$ 0.006	0.000 $\pm$ 0.006
$t\bar{t}\gamma$	0.000 $\pm$ 0.059	0.000 $\pm$ 0.059	0.000 $\pm$ 0.059	0.000 $\pm$ 0.059
$t\bar{t}W$	0.572 $\pm$ 0.025	0.733 $\pm$ 0.028	1.284 $\pm$ 0.038	2.590 $\pm$ 0.053
$t\bar{t}Z$	0.120 $\pm$ 0.009	0.159 $\pm$ 0.010	0.271 $\pm$ 0.013	0.549 $\pm$ 0.019
$WW\gamma$	0.000 $\pm$ 0.015	0.000 $\pm$ 0.015	0.000 $\pm$ 0.015	0.000 $\pm$ 0.015
WWW	0.001 $\pm$ 0.000	0.001 $\pm$ 0.000	0.001 $\pm$ 0.001	0.003 $\pm$ 0.001
WWZ	0.000 $\pm$ 0.000	0.000 $\pm$ 0.000	0.001 $\pm$ 0.001	0.001 $\pm$ 0.001
WZZ	0.000 $\pm$ 0.000	0.001 $\pm$ 0.000	0.001 $\pm$ 0.000	0.002 $\pm$ 0.001
ZZZ	0.000 $\pm$ 0.000	0.000 $\pm$ 0.000	0.000 $\pm$ 0.000	0.000 $\pm$ 0.000
Total MC	2.023 $\pm$ 0.166	1.072 $\pm$ 0.060	2.984 $\pm$ 0.163	6.079 $\pm$ 0.240
LM6	0.000 $\pm$ 0.000	0.186 $\pm$ 0.186	0.383 $\pm$ 0.275	0.569 $\pm$ 0.332
SF	1.13 $\pm$ 0.67	0.30 $\pm$ 0.20	1.92 $\pm$ 0.74	3.36 $\pm$ 1.02
DF	0.04 $\pm$ 0.12	0.02 $\pm$ 0.02	0.02 $\pm$ 0.09	0.08 $\pm$ 0.16
SF + DF	1.17 $\pm$ 0.63 $\pm$ 0.58	0.32 $\pm$ 0.20 $\pm$ 0.16	1.95 $\pm$ 0.72 $\pm$ 0.97	3.43 $\pm$ 0.98 $\pm$ 1.72
Charge Flips	0.509 $\pm$ 0.036 $\pm$ 0.102	- $\pm$ -	0.544 $\pm$ 0.032 $\pm$ 0.109	1.053 $\pm$ 0.048 $\pm$ 0.211
MC Pred	0.727 $\pm$ 0.029 $\pm$ 0.364	0.913 $\pm$ 0.031 $\pm$ 0.456	1.596 $\pm$ 0.042 $\pm$ 0.798	3.235 $\pm$ 0.059 $\pm$ 1.618
Total Pred	2.403 $\pm$ 0.633 $\pm$ 0.695	1.234 $\pm$ 0.199 $\pm$ 0.484	4.087 $\pm$ 0.725 $\pm$ 1.263	7.724 $\pm$ 0.983 $\pm$ 2.369
data	2	2	3	7

Table 10: Observed event yields in baseline ($\not{E}_T >$ 30 GeV, at least 2 jets with pT $>$ 40 GeV, and at least two of these jets b-tagged using SSVHEM) high-p_T (pT $>$ 20/20) dileptons compared to expectations from simulation alone, and from the data-driven methods. The upper part of the table is based on simulation only and is used only as a reference. The lower part is the main result of the analysis. The SF (DF) contributions are for events with one (two) fake leptons. The *MC Pred* contribution includes contributions from genuine same-sign lepton pairs (a sum of the rows from $V\gamma$ down to ZZZ). Entries with zero contributing events are reported with an uncertainty corresponding to one event. This uncertainty is not added to the total MC contribution. Systematic uncertainties (the second uncertainty if present) are displayed only for the final combined type of background, no systematic uncertainty is added for estimates with zero entries. Systematic uncertainties are 100% correlated among the channels.

Source	ee	$\mu\mu$	eμ	all
$t\bar{t} \to \ell\ell X$	0.380 $\pm$ 0.083	0.000 $\pm$ 0.199	0.414 $\pm$ 0.085	0.794 $\pm$ 0.119
$t\bar{t}$ other	0.000 $\pm$ 0.199	0.000 $\pm$ 0.199	0.000 $\pm$ 0.199	0.000 $\pm$ 0.199
$t\bar{t} \to \ell(b \to \ell)X$	0.038 $\pm$ 0.199	0.094 $\pm$ 0.199	0.025 $\pm$ 0.199	0.157 $\pm$ 0.055
$t\bar{t} \to \ell(\not b \to \ell)X$	0.343 $\pm$ 0.077	0.004 $\pm$ 0.199	0.321 $\pm$ 0.075	0.669 $\pm$ 0.108
t, s-channel	0.000 $\pm$ 0.057	0.000 $\pm$ 0.057	0.000 $\pm$ 0.057	0.000 $\pm$ 0.057
t, t-channel	0.000 $\pm$ 0.055	0.000 $\pm$ 0.055	0.000 $\pm$ 0.055	0.000 $\pm$ 0.055
tW	0.000 $\pm$ 0.045	0.000 $\pm$ 0.045	0.000 $\pm$ 0.045	0.000 $\pm$ 0.045
$Z \to ee$	0.000 $\pm$ 0.429	0.000 $\pm$ 0.429	0.000 $\pm$ 0.429	0.000 $\pm$ 0.429
$Z \to \mu\mu$	0.000 $\pm$ 0.429	0.000 $\pm$ 0.429	0.000 $\pm$ 0.429	0.000 $\pm$ 0.429
$Z \to \tau\tau$	0.000 $\pm$ 0.429	0.000 $\pm$ 0.429	0.000 $\pm$ 0.429	0.000 $\pm$ 0.429
W+jets	0.000 $\pm$ 1.808	0.000 $\pm$ 1.808	0.000 $\pm$ 1.808	0.000 $\pm$ 1.808
WW	0.000 $\pm$ 0.019	0.000 $\pm$ 0.019	0.000 $\pm$ 0.019	0.000 $\pm$ 0.019
Vγ	0.000 $\pm$ 0.248	0.000 $\pm$ 0.248	0.000 $\pm$ 0.248	0.000 $\pm$ 0.248
$W\gamma^* \to \ell\nu ee$	0.000 $\pm$ 0.097	0.000 $\pm$ 0.097	0.000 $\pm$ 0.097	0.000 $\pm$ 0.097
$W\gamma^* \to \ell\nu\mu\mu$	0.000 $\pm$ 0.075	0.000 $\pm$ 0.075	0.000 $\pm$ 0.075	0.000 $\pm$ 0.075
$W\gamma^* \to \ell\nu\tau\tau$	0.000 $\pm$ 0.028	0.000 $\pm$ 0.028	0.000 $\pm$ 0.028	0.000 $\pm$ 0.028
WZ	0.011 $\pm$ 0.006	0.005 $\pm$ 0.004	0.015 $\pm$ 0.007	0.031 $\pm$ 0.011
ZZ	0.000 $\pm$ 0.000	0.000 $\pm$ 0.000	0.001 $\pm$ 0.001	0.001 $\pm$ 0.001
dp$W^{\pm}W^{\pm}$	0.000 $\pm$ 0.004	0.000 $\pm$ 0.004	0.000 $\pm$ 0.004	0.000 $\pm$ 0.004
spW^-W^-	0.000 $\pm$ 0.001	0.000 $\pm$ 0.001	0.000 $\pm$ 0.001	0.000 $\pm$ 0.001
spW^+W^+	0.000 $\pm$ 0.006	0.000 $\pm$ 0.006	0.000 $\pm$ 0.006	0.000 $\pm$ 0.006
$t\bar{t}\gamma$	0.000 $\pm$ 0.059	0.000 $\pm$ 0.059	0.000 $\pm$ 0.059	0.000 $\pm$ 0.059
$t\bar{t}W$	0.422 $\pm$ 0.021	0.503 $\pm$ 0.023	0.898 $\pm$ 0.031	1.823 $\pm$ 0.044
$t\bar{t}Z$	0.058 $\pm$ 0.006	0.075 $\pm$ 0.007	0.134 $\pm$ 0.009	0.267 $\pm$ 0.013
$WW\gamma$	0.000 $\pm$ 0.015	0.000 $\pm$ 0.015	0.000 $\pm$ 0.015	0.000 $\pm$ 0.015
WWW	0.000 $\pm$ 0.000	0.001 $\pm$ 0.000	0.001 $\pm$ 0.000	0.002 $\pm$ 0.001
WWZ	0.000 $\pm$ 0.000	0.000 $\pm$ 0.000	0.000 $\pm$ 0.000	0.000 $\pm$ 0.000
WZZ	0.000 $\pm$ 0.000	0.001 $\pm$ 0.000	0.000 $\pm$ 0.000	0.001 $\pm$ 0.001
ZZZ	0.000 $\pm$ 0.000	0.000 $\pm$ 0.000	0.000 $\pm$ 0.000	0.000 $\pm$ 0.000
Total MC	1.254 $\pm$ 0.119	0.683 $\pm$ 0.048	1.809 $\pm$ 0.120	3.746 $\pm$ 0.176
LM6	0.000 $\pm$ 0.000	0.186 $\pm$ 0.186	0.224 $\pm$ 0.224	0.410 $\pm$ 0.291
SF	0.06 $\pm$ 0.50	0.30 $\pm$ 0.20	1.32 $\pm$ 0.66	1.69 $\pm$ 0.85
DF	0.04 $\pm$ 0.12	0.02 $\pm$ 0.02	0.02 $\pm$ 0.09	0.08 $\pm$ 0.16
SF + DF	0.10 $\pm$ 0.45 $\pm$ 0.05	0.32 $\pm$ 0.20 $\pm$ 0.16	1.34 $\pm$ 0.64 $\pm$ 0.67	1.76 $\pm$ 0.80 $\pm$ 0.88
Charge Flips	0.255 $\pm$ 0.018 $\pm$ 0.051	- $\pm$ -	0.272 $\pm$ 0.016 $\pm$ 0.054	0.527 $\pm$ 0.024 $\pm$ 0.105
MC Pred	0.492 $\pm$ 0.023 $\pm$ 0.246	0.585 $\pm$ 0.024 $\pm$ 0.293	1.049 $\pm$ 0.034 $\pm$ 0.525	2.127 $\pm$ 0.047 $\pm$ 1.064
Total Pred	0.848 $\pm$ 0.450 $\pm$ 0.256	0.906 $\pm$ 0.198 $\pm$ 0.334	2.663 $\pm$ 0.637 $\pm$ 0.853	4.417 $\pm$ 0.804 $\pm$ 1.385
data	2	1	2	5

Table 11: Observed event yields in the "++" search region (baseline selection with both leptons positively charged) compared to expectations from simulation alone, and from the data-driven methods. The upper part of the table is based on simulation only and is used only as a reference. The lower part is the main result of the analysis. The SF (DF) contributions are for events with one (two) fake leptons. The *MC Pred* contribution includes contributions from genuine same-sign lepton pairs (a sum of the rows from $V\gamma$ down to ZZZ). Entries with zero contributing events are reported with an uncertainty corresponding to one event. This uncertainty is not added to the total MC contribution. Systematic uncertainties (the second uncertainty if present) are displayed only for the final combined type of background, no systematic uncertainty is added for estimates with zero entries. Systematic uncertainties are 100% correlated among the channels.

Source	ee	$\mu\mu$	eμ	all
$t\bar{t} \to \ell\ell X$	0.017 $\pm$ 0.199	0.000 $\pm$ 0.199	0.017 $\pm$ 0.199	0.034 $\pm$ 0.199
$t\bar{t}$ other	0.000 $\pm$ 0.199	0.000 $\pm$ 0.199	0.000 $\pm$ 0.199	0.000 $\pm$ 0.199
$t\bar{t} \to \ell(b \to \ell)X$	0.000 $\pm$ 0.199	0.020 $\pm$ 0.199	0.000 $\pm$ 0.199	0.020 $\pm$ 0.199
$t\bar{t} \to \ell(\not{b} \to \ell)X$	0.059 $\pm$ 0.199	0.000 $\pm$ 0.199	0.099 $\pm$ 0.199	0.157 $\pm$ 0.050
t, s-channel	0.000 $\pm$ 0.057	0.000 $\pm$ 0.057	0.000 $\pm$ 0.057	0.000 $\pm$ 0.057
t, t-channel	0.000 $\pm$ 0.055	0.000 $\pm$ 0.055	0.000 $\pm$ 0.055	0.000 $\pm$ 0.055
tW	0.000 $\pm$ 0.045	0.000 $\pm$ 0.045	0.000 $\pm$ 0.045	0.000 $\pm$ 0.045
$Z \to ee$	0.000 $\pm$ 0.429	0.000 $\pm$ 0.429	0.000 $\pm$ 0.429	0.000 $\pm$ 0.429
$Z \to \mu\mu$	0.000 $\pm$ 0.429	0.000 $\pm$ 0.429	0.000 $\pm$ 0.429	0.000 $\pm$ 0.429
$Z \to \tau\tau$	0.000 $\pm$ 0.429	0.000 $\pm$ 0.429	0.000 $\pm$ 0.429	0.000 $\pm$ 0.429
W+jets	0.000 $\pm$ 1.808	0.000 $\pm$ 1.808	0.000 $\pm$ 1.808	0.000 $\pm$ 1.808
WW	0.000 $\pm$ 0.019	0.000 $\pm$ 0.019	0.000 $\pm$ 0.019	0.000 $\pm$ 0.019
Vγ	0.000 $\pm$ 0.248	0.000 $\pm$ 0.248	0.000 $\pm$ 0.248	0.000 $\pm$ 0.248
$W\gamma^* \to \ell\nu ee$	0.000 $\pm$ 0.097	0.000 $\pm$ 0.097	0.000 $\pm$ 0.097	0.000 $\pm$ 0.097
$W\gamma^* \to \ell\nu\mu\mu$	0.000 $\pm$ 0.075	0.000 $\pm$ 0.075	0.000 $\pm$ 0.075	0.000 $\pm$ 0.075
$W\gamma^* \to \ell\nu\tau\tau$	0.000 $\pm$ 0.028	0.000 $\pm$ 0.028	0.000 $\pm$ 0.028	0.000 $\pm$ 0.028
WZ	0.010 $\pm$ 0.007	0.001 $\pm$ 0.003	0.000 $\pm$ 0.003	0.011 $\pm$ 0.007
ZZ	0.000 $\pm$ 0.000	0.000 $\pm$ 0.000	0.001 $\pm$ 0.001	0.001 $\pm$ 0.001
dp$W^{\pm}W^{\pm}$	0.000 $\pm$ 0.004	0.000 $\pm$ 0.004	0.000 $\pm$ 0.004	0.000 $\pm$ 0.004
sp$W^{-}W^{-}$	0.000 $\pm$ 0.001	0.000 $\pm$ 0.001	0.001 $\pm$ 0.001	0.001 $\pm$ 0.001
sp$W^{+}W^{+}$	0.000 $\pm$ 0.006	0.000 $\pm$ 0.006	0.000 $\pm$ 0.006	0.000 $\pm$ 0.006
$t\bar{t}\gamma$	0.000 $\pm$ 0.059	0.000 $\pm$ 0.059	0.000 $\pm$ 0.059	0.000 $\pm$ 0.059
$t\bar{t}W$	0.098 $\pm$ 0.010	0.121 $\pm$ 0.011	0.244 $\pm$ 0.016	0.463 $\pm$ 0.022
$t\bar{t}Z$	0.016 $\pm$ 0.003	0.023 $\pm$ 0.004	0.041 $\pm$ 0.005	0.080 $\pm$ 0.007
$WW\gamma$	0.000 $\pm$ 0.015	0.000 $\pm$ 0.015	0.000 $\pm$ 0.015	0.000 $\pm$ 0.015
WWW	0.000 $\pm$ 0.000	0.000 $\pm$ 0.000	0.000 $\pm$ 0.000	0.001 $\pm$ 0.000
WWZ	0.000 $\pm$ 0.000	0.000 $\pm$ 0.000	0.000 $\pm$ 0.000	0.000 $\pm$ 0.000
WZZ	0.000 $\pm$ 0.000	0.000 $\pm$ 0.000	0.000 $\pm$ 0.000	0.000 $\pm$ 0.000
ZZZ	0.000 $\pm$ 0.000	0.000 $\pm$ 0.000	0.000 $\pm$ 0.000	0.000 $\pm$ 0.000
Total MC	0.199 $\pm$ 0.035	0.165 $\pm$ 0.023	0.404 $\pm$ 0.047	0.768 $\pm$ 0.063
LM6	0.000 $\pm$ 0.000	0.186 $\pm$ 0.186	0.383 $\pm$ 0.275	0.569 $\pm$ 0.332
SF	0.00 $\pm$ 0.58	0.00 $\pm$ 0.37	0.32 $\pm$ 0.57	0.32 $\pm$ 0.57
DF	0.00 $\pm$ 0.14	0.00 $\pm$ 0.10	0.00 $\pm$ 0.16	0.00 $\pm$ 0.16
SF + DF	0.00 $\pm$ 0.50 $\pm$ 0.00	0.00 $\pm$ 0.31 $\pm$ 0.00	0.32 $\pm$ 0.47 $\pm$ 0.16	0.32 $\pm$ 0.47 $\pm$ 0.16
Charge Flips	0.023 $\pm$ 0.007 $\pm$ 0.005	- $\pm$ -	0.022 $\pm$ 0.006 $\pm$ 0.004	0.045 $\pm$ 0.009 $\pm$ 0.009
MC Pred	0.123 $\pm$ 0.013 $\pm$ 0.062	0.145 $\pm$ 0.012 $\pm$ 0.073	0.288 $\pm$ 0.017 $\pm$ 0.144	0.557 $\pm$ 0.024 $\pm$ 0.278
Total Pred	0.146 $\pm$ 0.501 $\pm$ 0.062	0.145 $\pm$ 0.315 $\pm$ 0.073	0.635 $\pm$ 0.474 $\pm$ 0.217	0.926 $\pm$ 0.474 $\pm$ 0.322
data	1	0	1	2

Table 12: Observed event yields in the low-H_T high-$\not\!\!E_T$ region (H_T > 200 GeV, $\not\!\!E_T$> 120 GeV) compared to expectations from simulation alone, and from the data-driven methods. The upper part of the table is based on simulation only and is used only as a reference. The lower part is the main result of the analysis. The SF (DF) contributions are for events with one (two) fake leptons. The *MC Pred* contribution includes contributions from genuine same-sign lepton pairs (a sum of the rows from $V\gamma$ down to ZZZ). Entries with zero contributing events are reported with an uncertainty corresponding to one event. This uncertainty is not added to the total MC contribution. Systematic uncertainties (the second uncertainty if present) are displayed only for the final combined type of background, no systematic uncertainty is added for estimates with zero entries. Systematic uncertainties are 100% correlated among the channels.

Source	ee	$\mu\mu$	eμ	all
$t\bar{t} \to \ell\ell X$	0.235 ± 0.065	0.000 ± 0.199	0.159 ± 0.054	0.394 ± 0.084
$t\bar{t}$ other	0.000 ± 0.199	0.000 ± 0.199	0.000 ± 0.199	0.000 ± 0.199
$t\bar{t} \to \ell(b \to \ell)X$	0.042 ± 0.199	0.054 ± 0.199	0.044 ± 0.199	0.140 ± 0.052
$t\bar{t} \to \ell(\not{b} \to \ell)X$	0.270 ± 0.067	0.016 ± 0.199	0.386 ± 0.086	0.672 ± 0.110
t, s-channel	0.000 ± 0.057	0.000 ± 0.057	0.000 ± 0.057	0.000 ± 0.057
t, t-channel	0.000 ± 0.055	0.000 ± 0.055	0.000 ± 0.055	0.000 ± 0.055
tW	0.000 ± 0.045	0.000 ± 0.045	0.016 ± 0.045	0.016 ± 0.045
$Z \to ee$	0.000 ± 0.429	0.000 ± 0.429	0.000 ± 0.429	0.000 ± 0.429
$Z \to \mu\mu$	0.000 ± 0.429	0.000 ± 0.429	0.000 ± 0.429	0.000 ± 0.429
$Z \to \tau\tau$	0.000 ± 0.429	0.000 ± 0.429	0.000 ± 0.429	0.000 ± 0.429
W+jets	0.000 ± 1.808	0.000 ± 1.808	0.000 ± 1.808	0.000 ± 1.808
WW	0.000 ± 0.019	0.000 ± 0.019	0.000 ± 0.019	0.000 ± 0.019
Vγ	0.000 ± 0.248	0.000 ± 0.248	0.000 ± 0.248	0.000 ± 0.248
$W\gamma^* \to \ell\nu ee$	0.000 ± 0.097	0.000 ± 0.097	0.000 ± 0.097	0.000 ± 0.097
$W\gamma^* \to \ell\nu\mu\mu$	0.000 ± 0.075	0.000 ± 0.075	0.000 ± 0.075	0.000 ± 0.075
$W\gamma^* \to \ell\nu\tau\tau$	0.000 ± 0.028	0.000 ± 0.028	0.000 ± 0.028	0.000 ± 0.028
WZ	0.019 ± 0.009	0.013 ± 0.007	0.010 ± 0.006	0.042 ± 0.013
ZZ	0.000 ± 0.000	0.000 ± 0.000	0.001 ± 0.001	0.001 ± 0.001
dp$W^\pm W^\pm$	0.000 ± 0.004	0.000 ± 0.004	0.000 ± 0.004	0.000 ± 0.004
spW^-W^-	0.000 ± 0.001	0.000 ± 0.001	0.003 ± 0.002	0.003 ± 0.002
spW^+W^+	0.000 ± 0.006	0.000 ± 0.006	0.000 ± 0.006	0.000 ± 0.006
$t\bar{t}\gamma$	0.000 ± 0.059	0.000 ± 0.059	0.000 ± 0.059	0.000 ± 0.059
$t\bar{t}W$	0.376 ± 0.020	0.430 ± 0.021	0.768 ± 0.029	1.574 ± 0.041
$t\bar{t}Z$	0.066 ± 0.007	0.099 ± 0.008	0.162 ± 0.010	0.327 ± 0.015
$WW\gamma$	0.000 ± 0.015	0.000 ± 0.015	0.000 ± 0.015	0.000 ± 0.015
WWW	0.000 ± 0.000	0.000 ± 0.000	0.001 ± 0.001	0.002 ± 0.001
WWZ	0.000 ± 0.000	0.000 ± 0.000	0.001 ± 0.001	0.001 ± 0.001
WZZ	0.000 ± 0.000	0.000 ± 0.000	0.000 ± 0.000	0.001 ± 0.000
ZZZ	0.000 ± 0.000	0.000 ± 0.000	0.000 ± 0.000	0.000 ± 0.000
Total MC	1.008 ± 0.100	0.612 ± 0.041	1.552 ± 0.112	3.172 ± 0.156
LM6	0.000 ± 0.000	0.186 ± 0.186	0.383 ± 0.275	0.569 ± 0.332
SF	0.51 ± 0.59	0.00 ± 0.37	0.98 ± 0.67	1.49 ± 0.85
DF	0.00 ± 0.14	0.00 ± 0.10	0.00 ± 0.16	0.00 ± 0.16
SF + DF	0.51 ± 0.51 ± 0.25	0.00 ± 0.31 ± 0.00	0.98 ± 0.60 ± 0.49	1.49 ± 0.79 ± 0.75
Charge Flips	0.122 ± 0.017 ± 0.024	- ± -	0.158 ± 0.017 ± 0.032	0.281 ± 0.024 ± 0.056
MC Pred	0.462 ± 0.024 ± 0.231	0.542 ± 0.024 ± 0.271	0.948 ± 0.031 ± 0.474	1.952 ± 0.046 ± 0.976
Total Pred	1.093 ± 0.512 ± 0.345	0.542 ± 0.315 ± 0.271	2.087 ± 0.597 ± 0.683	3.723 ± 0.787 ± 1.229
data	2	1	2	5

Table 13: Observed event yields in the low-H_T low-$\not{E}_T$ region ($H_T > 200$ GeV, $\not{E}_T > 50$ GeV) compared to expectations from simulation alone, and from the data-driven methods. The upper part of the table is based on simulation only and is used only as a reference. The lower part is the main result of the analysis. The SF (DF) contributions are for events with one (two) fake leptons. The *MC Pred* contribution includes contributions from genuine same-sign lepton pairs (a sum of the rows from $V\gamma$ down to ZZZ). Entries with zero contributing events are reported with an uncertainty corresponding to one event. This uncertainty is not added to the total MC contribution. Systematic uncertainties (the second uncertainty if present) are displayed only for the final combined type of background, no systematic uncertainty is added for estimates with zero entries. Systematic uncertainties are 100% correlated among the channels.

Source	ee	$\mu\mu$	eμ	all
$t\bar{t} \to \ell\ell X$	0.067 $\pm$ 0.199	0.000 $\pm$ 0.199	0.078 $\pm$ 0.199	0.146 $\pm$ 0.050
$t\bar{t}$ other	0.000 $\pm$ 0.199	0.000 $\pm$ 0.199	0.000 $\pm$ 0.199	0.000 $\pm$ 0.199
$t\bar{t} \to \ell(b \to \ell)X$	0.025 $\pm$ 0.199	0.040 $\pm$ 0.199	0.019 $\pm$ 0.199	0.085 $\pm$ 0.199
$t\bar{t} \to \ell(\not{b} \to \ell)X$	0.109 $\pm$ 0.043	0.016 $\pm$ 0.199	0.188 $\pm$ 0.060	0.313 $\pm$ 0.076
t, s-channel	0.000 $\pm$ 0.057	0.000 $\pm$ 0.057	0.000 $\pm$ 0.057	0.000 $\pm$ 0.057
t, t-channel	0.000 $\pm$ 0.055	0.000 $\pm$ 0.055	0.000 $\pm$ 0.055	0.000 $\pm$ 0.055
tW	0.000 $\pm$ 0.045	0.000 $\pm$ 0.045	0.000 $\pm$ 0.045	0.000 $\pm$ 0.045
$Z \to ee$	0.000 $\pm$ 0.429	0.000 $\pm$ 0.429	0.000 $\pm$ 0.429	0.000 $\pm$ 0.429
$Z \to \mu\mu$	0.000 $\pm$ 0.429	0.000 $\pm$ 0.429	0.000 $\pm$ 0.429	0.000 $\pm$ 0.429
$Z \to \tau\tau$	0.000 $\pm$ 0.429	0.000 $\pm$ 0.429	0.000 $\pm$ 0.429	0.000 $\pm$ 0.429
W+jets	0.000 $\pm$ 1.808	0.000 $\pm$ 1.808	0.000 $\pm$ 1.808	0.000 $\pm$ 1.808
WW	0.000 $\pm$ 0.019	0.000 $\pm$ 0.019	0.000 $\pm$ 0.019	0.000 $\pm$ 0.019
Vγ	0.000 $\pm$ 0.248	0.000 $\pm$ 0.248	0.000 $\pm$ 0.248	0.000 $\pm$ 0.248
$W\gamma^* \to \ell\nu ee$	0.000 $\pm$ 0.097	0.000 $\pm$ 0.097	0.000 $\pm$ 0.097	0.000 $\pm$ 0.097
$W\gamma^* \to \ell\nu\mu\mu$	0.000 $\pm$ 0.075	0.000 $\pm$ 0.075	0.000 $\pm$ 0.075	0.000 $\pm$ 0.075
$W\gamma^* \to \ell\nu\tau\tau$	0.000 $\pm$ 0.028	0.000 $\pm$ 0.028	0.000 $\pm$ 0.028	0.000 $\pm$ 0.028
WZ	0.009 $\pm$ 0.006	0.001 $\pm$ 0.003	0.006 $\pm$ 0.004	0.016 $\pm$ 0.008
ZZ	0.000 $\pm$ 0.000	0.000 $\pm$ 0.000	0.000 $\pm$ 0.000	0.000 $\pm$ 0.000
dp$W^\pm W^\pm$	0.000 $\pm$ 0.004	0.000 $\pm$ 0.004	0.000 $\pm$ 0.004	0.000 $\pm$ 0.004
spW^-W^-	0.000 $\pm$ 0.001	0.000 $\pm$ 0.001	0.001 $\pm$ 0.001	0.001 $\pm$ 0.001
spW^+W^+	0.000 $\pm$ 0.006	0.000 $\pm$ 0.006	0.000 $\pm$ 0.006	0.000 $\pm$ 0.006
$t\bar{t}\gamma$	0.000 $\pm$ 0.059	0.000 $\pm$ 0.059	0.000 $\pm$ 0.059	0.000 $\pm$ 0.059
$t\bar{t}W$	0.201 $\pm$ 0.015	0.214 $\pm$ 0.015	0.414 $\pm$ 0.021	0.829 $\pm$ 0.030
$t\bar{t}Z$	0.037 $\pm$ 0.005	0.055 $\pm$ 0.006	0.094 $\pm$ 0.008	0.187 $\pm$ 0.011
$WW\gamma$	0.000 $\pm$ 0.015	0.000 $\pm$ 0.015	0.000 $\pm$ 0.015	0.000 $\pm$ 0.015
WWW	0.000 $\pm$ 0.000	0.000 $\pm$ 0.000	0.001 $\pm$ 0.001	0.002 $\pm$ 0.001
WWZ	0.000 $\pm$ 0.000	0.000 $\pm$ 0.000	0.000 $\pm$ 0.000	0.000 $\pm$ 0.000
WZZ	0.000 $\pm$ 0.000	0.000 $\pm$ 0.000	0.000 $\pm$ 0.000	0.000 $\pm$ 0.000
ZZZ	0.000 $\pm$ 0.000	0.000 $\pm$ 0.000	0.000 $\pm$ 0.000	0.000 $\pm$ 0.000
Total MC	0.449 $\pm$ 0.061	0.327 $\pm$ 0.034	0.803 $\pm$ 0.078	1.579 $\pm$ 0.105
LM6	0.000 $\pm$ 0.000	0.186 $\pm$ 0.186	0.383 $\pm$ 0.275	0.569 $\pm$ 0.332
SF	0.27 $\pm$ 0.54	0.00 $\pm$ 0.37	0.54 $\pm$ 0.59	0.81 $\pm$ 0.74
DF	0.00 $\pm$ 0.14	0.00 $\pm$ 0.10	0.00 $\pm$ 0.16	0.00 $\pm$ 0.16
SF + DF	0.27 $\pm$ 0.45 $\pm$ 0.14	0.00 $\pm$ 0.31 $\pm$ 0.00	0.54 $\pm$ 0.50 $\pm$ 0.27	0.81 $\pm$ 0.67 $\pm$ 0.40
Charge Flips	0.049 $\pm$ 0.011 $\pm$ 0.010	- $\pm$ -	0.069 $\pm$ 0.012 $\pm$ 0.014	0.118 $\pm$ 0.016 $\pm$ 0.024
MC Pred	0.247 $\pm$ 0.017 $\pm$ 0.124	0.271 $\pm$ 0.016 $\pm$ 0.136	0.518 $\pm$ 0.023 $\pm$ 0.259	1.036 $\pm$ 0.033 $\pm$ 0.518
Total Pred	0.569 $\pm$ 0.453 $\pm$ 0.185	0.271 $\pm$ 0.315 $\pm$ 0.136	1.122 $\pm$ 0.496 $\pm$ 0.373	1.962 $\pm$ 0.672 $\pm$ 0.658
data	1	1	0	2

Table 14: Observed event yields in the high-H_T low-$\not{E}_T$ region ($H_T > 320$ GeV, $\not{E}_T > 50$ GeV) compared to expectations from simulation alone, and from the data-driven methods. The upper part of the table is based on simulation only and is used only as a reference. The lower part is the main result of the analysis. The SF (DF) contributions are for events with one (two) fake leptons. The *MC Pred* contribution includes contributions from genuine same-sign lepton pairs (a sum of the rows from $V\gamma$ down to ZZZ). Entries with zero contributing events are reported with an uncertainty corresponding to one event. This uncertainty is not added to the total MC contribution. Systematic uncertainties (the second uncertainty if present) are displayed only for the final combined type of background, no systematic uncertainty is added for estimates with zero entries. Systematic uncertainties are 100% correlated among the channels.

Source	ee	$\mu\mu$	eμ	all
$t\bar{t} \rightarrow \ell\ell X$	0.000 $\pm$ 0.199	0.000 $\pm$ 0.199	0.017 $\pm$ 0.199	0.017 $\pm$ 0.199
$t\bar{t}$ other	0.000 $\pm$ 0.199	0.000 $\pm$ 0.199	0.000 $\pm$ 0.199	0.000 $\pm$ 0.199
$t\bar{t} \rightarrow \ell(b \rightarrow \ell)X$	0.000 $\pm$ 0.199	0.020 $\pm$ 0.199	0.000 $\pm$ 0.199	0.020 $\pm$ 0.199
$t\bar{t} \rightarrow \ell(\not{b} \rightarrow \ell)X$	0.033 $\pm$ 0.199	0.000 $\pm$ 0.199	0.050 $\pm$ 0.199	0.082 $\pm$ 0.199
t, s-channel	0.000 $\pm$ 0.057	0.000 $\pm$ 0.057	0.000 $\pm$ 0.057	0.000 $\pm$ 0.057
t, t-channel	0.000 $\pm$ 0.055	0.000 $\pm$ 0.055	0.000 $\pm$ 0.055	0.000 $\pm$ 0.055
tW	0.000 $\pm$ 0.045	0.000 $\pm$ 0.045	0.000 $\pm$ 0.045	0.000 $\pm$ 0.045
$Z \rightarrow ee$	0.000 $\pm$ 0.429	0.000 $\pm$ 0.429	0.000 $\pm$ 0.429	0.000 $\pm$ 0.429
$Z \rightarrow \mu\mu$	0.000 $\pm$ 0.429	0.000 $\pm$ 0.429	0.000 $\pm$ 0.429	0.000 $\pm$ 0.429
$Z \rightarrow \tau\tau$	0.000 $\pm$ 0.429	0.000 $\pm$ 0.429	0.000 $\pm$ 0.429	0.000 $\pm$ 0.429
W+jets	0.000 $\pm$ 1.808	0.000 $\pm$ 1.808	0.000 $\pm$ 1.808	0.000 $\pm$ 1.808
WW	0.000 $\pm$ 0.019	0.000 $\pm$ 0.019	0.000 $\pm$ 0.019	0.000 $\pm$ 0.019
Vγ	0.000 $\pm$ 0.248	0.000 $\pm$ 0.248	0.000 $\pm$ 0.248	0.000 $\pm$ 0.248
$W\gamma^* \rightarrow \ell\nu ee$	0.000 $\pm$ 0.097	0.000 $\pm$ 0.097	0.000 $\pm$ 0.097	0.000 $\pm$ 0.097
$W\gamma^* \rightarrow \ell\nu\mu\mu$	0.000 $\pm$ 0.075	0.000 $\pm$ 0.075	0.000 $\pm$ 0.075	0.000 $\pm$ 0.075
$W\gamma^* \rightarrow \ell\nu\tau\tau$	0.000 $\pm$ 0.028	0.000 $\pm$ 0.028	0.000 $\pm$ 0.028	0.000 $\pm$ 0.028
WZ	0.004 $\pm$ 0.004	0.001 $\pm$ 0.003	0.000 $\pm$ 0.003	0.006 $\pm$ 0.005
ZZ	0.000 $\pm$ 0.000	0.000 $\pm$ 0.000	0.000 $\pm$ 0.000	0.000 $\pm$ 0.000
dp$W^{\pm}W^{\pm}$	0.000 $\pm$ 0.004	0.000 $\pm$ 0.004	0.000 $\pm$ 0.004	0.000 $\pm$ 0.004
sp$W^{-}W^{-}$	0.000 $\pm$ 0.001	0.000 $\pm$ 0.001	0.001 $\pm$ 0.001	0.001 $\pm$ 0.001
sp$W^{+}W^{+}$	0.000 $\pm$ 0.006	0.000 $\pm$ 0.006	0.000 $\pm$ 0.006	0.000 $\pm$ 0.006
$t\bar{t}\gamma$	0.000 $\pm$ 0.059	0.000 $\pm$ 0.059	0.000 $\pm$ 0.059	0.000 $\pm$ 0.059
$t\bar{t}W$	0.070 $\pm$ 0.009	0.080 $\pm$ 0.009	0.168 $\pm$ 0.013	0.317 $\pm$ 0.018
$t\bar{t}Z$	0.013 $\pm$ 0.003	0.015 $\pm$ 0.003	0.032 $\pm$ 0.005	0.060 $\pm$ 0.006
$WW\gamma$	0.000 $\pm$ 0.015	0.000 $\pm$ 0.015	0.000 $\pm$ 0.015	0.000 $\pm$ 0.015
WWW	0.000 $\pm$ 0.000	0.000 $\pm$ 0.000	0.000 $\pm$ 0.000	0.001 $\pm$ 0.000
WWZ	0.000 $\pm$ 0.000	0.000 $\pm$ 0.000	0.000 $\pm$ 0.000	0.000 $\pm$ 0.000
WZZ	0.000 $\pm$ 0.000	0.000 $\pm$ 0.000	0.000 $\pm$ 0.000	0.000 $\pm$ 0.000
ZZZ	0.000 $\pm$ 0.000	0.000 $\pm$ 0.000	0.000 $\pm$ 0.000	0.000 $\pm$ 0.000
Total MC	0.120 $\pm$ 0.025	0.116 $\pm$ 0.022	0.269 $\pm$ 0.036	0.504 $\pm$ 0.049
LM6	0.000 $\pm$ 0.000	0.186 $\pm$ 0.186	0.383 $\pm$ 0.275	0.569 $\pm$ 0.332
SF	0.00 $\pm$ 0.58	0.00 $\pm$ 0.37	0.15 $\pm$ 0.54	0.15 $\pm$ 0.54
DF	0.00 $\pm$ 0.14	0.00 $\pm$ 0.10	0.00 $\pm$ 0.16	0.00 $\pm$ 0.16
SF + DF	0.00 $\pm$ 0.50 $\pm$ 0.00	0.00 $\pm$ 0.31 $\pm$ 0.00	0.15 $\pm$ 0.44 $\pm$ 0.07	0.15 $\pm$ 0.44 $\pm$ 0.07
Charge Flips	0.014 $\pm$ 0.006 $\pm$ 0.003	- $\pm$ -	0.011 $\pm$ 0.005 $\pm$ 0.002	0.026 $\pm$ 0.008 $\pm$ 0.005
MC Pred	0.087 $\pm$ 0.010 $\pm$ 0.044	0.096 $\pm$ 0.010 $\pm$ 0.048	0.202 $\pm$ 0.014 $\pm$ 0.101	0.385 $\pm$ 0.020 $\pm$ 0.193
Total Pred	0.101 $\pm$ 0.501 $\pm$ 0.044	0.096 $\pm$ 0.315 $\pm$ 0.048	0.363 $\pm$ 0.438 $\pm$ 0.126	0.560 $\pm$ 0.438 $\pm$ 0.207
data	0	0	0	0

Table 15: Observed event yields in the high-H_T high-$\not{E}_T$ region ($H_T > 320$ GeV, $\not{E}_T > 120$ GeV) compared to expectations from simulation alone, and from the data-driven methods. The upper part of the table is based on simulation only and is used only as a reference. The lower part is the main result of the analysis. The SF (DF) contributions are for events with one (two) fake leptons. The *MC Pred* contribution includes contributions from genuine same-sign lepton pairs (a sum of the rows from $V\gamma$ down to ZZZ). Entries with zero contributing events are reported with an uncertainty corresponding to one event. This uncertainty is not added to the total MC contribution. Systematic uncertainties (the second uncertainty if present) are displayed only for the final combined type of background, no systematic uncertainty is added for estimates with zero entries. Systematic uncertainties are 100% correlated among the channels.

Source	ee	$\mu\mu$	eμ	all
$t\bar{t} \rightarrow \ell\ell X$	0.000 ± 0.199	0.000 ± 0.199	0.000 ± 0.199	0.000 ± 0.199
$t\bar{t}$ other	0.000 ± 0.199	0.000 ± 0.199	0.000 ± 0.199	0.000 ± 0.199
$t\bar{t} \rightarrow \ell(b \rightarrow \ell)X$	0.000 ± 0.199	0.020 ± 0.199	0.000 ± 0.199	0.020 ± 0.199
$t\bar{t} \rightarrow \ell(\not{b} \rightarrow \ell)X$	0.000 ± 0.199	0.000 ± 0.199	0.019 ± 0.199	0.019 ± 0.199
t, s-channel	0.000 ± 0.057	0.000 ± 0.057	0.000 ± 0.057	0.000 ± 0.057
t, t-channel	0.000 ± 0.055	0.000 ± 0.055	0.000 ± 0.055	0.000 ± 0.055
tW	0.000 ± 0.045	0.000 ± 0.045	0.000 ± 0.045	0.000 ± 0.045
$Z \rightarrow ee$	0.000 ± 0.429	0.000 ± 0.429	0.000 ± 0.429	0.000 ± 0.429
$Z \rightarrow \mu\mu$	0.000 ± 0.429	0.000 ± 0.429	0.000 ± 0.429	0.000 ± 0.429
$Z \rightarrow \tau\tau$	0.000 ± 0.429	0.000 ± 0.429	0.000 ± 0.429	0.000 ± 0.429
W+jets	0.000 ± 1.808	0.000 ± 1.808	0.000 ± 1.808	0.000 ± 1.808
WW	0.000 ± 0.019	0.000 ± 0.019	0.000 ± 0.019	0.000 ± 0.019
Vγ	0.000 ± 0.248	0.000 ± 0.248	0.000 ± 0.248	0.000 ± 0.248
$W\gamma^* \rightarrow \ell\nu ee$	0.000 ± 0.097	0.000 ± 0.097	0.000 ± 0.097	0.000 ± 0.097
$W\gamma^* \rightarrow \ell\nu\mu\mu$	0.000 ± 0.075	0.000 ± 0.075	0.000 ± 0.075	0.000 ± 0.075
$W\gamma^* \rightarrow \ell\nu\tau\tau$	0.000 ± 0.028	0.000 ± 0.028	0.000 ± 0.028	0.000 ± 0.028
WZ	0.005 ± 0.005	0.000 ± 0.003	0.000 ± 0.003	0.005 ± 0.005
ZZ	0.000 ± 0.000	0.000 ± 0.000	0.000 ± 0.000	0.000 ± 0.000
dp$W^{\pm}W^{\pm}$	0.000 ± 0.004	0.000 ± 0.004	0.000 ± 0.004	0.000 ± 0.004
sp$W^{-}W^{-}$	0.000 ± 0.001	0.000 ± 0.001	0.000 ± 0.001	0.000 ± 0.001
sp$W^{+}W^{+}$	0.000 ± 0.006	0.000 ± 0.006	0.000 ± 0.006	0.000 ± 0.006
$t\bar{t}\gamma$	0.000 ± 0.059	0.000 ± 0.059	0.000 ± 0.059	0.000 ± 0.059
$t\bar{t}W$	0.014 ± 0.003	0.029 ± 0.006	0.043 ± 0.007	0.086 ± 0.010
$t\bar{t}Z$	0.003 ± 0.001	0.006 ± 0.002	0.014 ± 0.003	0.023 ± 0.004
$WW\gamma$	0.000 ± 0.015	0.000 ± 0.015	0.000 ± 0.015	0.000 ± 0.015
WWW	0.000 ± 0.000	0.000 ± 0.000	0.000 ± 0.000	0.000 ± 0.000
WWZ	0.000 ± 0.000	0.000 ± 0.000	0.000 ± 0.000	0.000 ± 0.000
WZZ	0.000 ± 0.000	0.000 ± 0.000	0.000 ± 0.000	0.000 ± 0.000
ZZZ	0.000 ± 0.000	0.000 ± 0.000	0.000 ± 0.000	0.000 ± 0.000
Total MC	0.021 ± 0.006	0.055 ± 0.021	0.076 ± 0.021	0.152 ± 0.030
LM6	0.000 ± 0.000	0.000 ± 0.000	0.000 ± 0.000	0.000 ± 0.000
SF	0.00 ± 0.58	0.00 ± 0.37	0.15 ± 0.54	0.15 ± 0.54
DF	0.00 ± 0.14	0.00 ± 0.10	0.00 ± 0.16	0.00 ± 0.16
SF + DF	0.00 ± 0.50 ± 0.00	0.00 ± 0.31 ± 0.00	0.15 ± 0.44 ± 0.07	0.15 ± 0.44 ± 0.07
Charge Flips	0.003 ± 0.002 ± 0.001	- ± -	0.005 ± 0.002 ± 0.001	0.008 ± 0.003 ± 0.002
MC Pred	0.021 ± 0.006 ± 0.011	0.036 ± 0.006 ± 0.018	0.057 ± 0.007 ± 0.028	0.113 ± 0.011 ± 0.057
Total Pred	0.024 ± 0.501 ± 0.011	0.036 ± 0.315 ± 0.018	0.211 ± 0.438 ± 0.080	0.270 ± 0.438 ± 0.094
data	0	0	0	0

Table 16: Observed event yields in the low-H_T low-$\not{E}_T$ region ($H_T > 200$ GeV, $\not{E}_T > 50$ GeV) requiring at least three b-tagged jets compared to expectations from simulation alone, and from the data-driven methods. The upper part of the table is based on simulation only and is used only as a reference. The lower part is the main result of the analysis. The SF (DF) contributions are for events with one (two) fake leptons. The *MC Pred* contribution includes contributions from genuine same-sign lepton pairs (a sum of the rows from $V\gamma$ down to ZZZ). Entries with zero contributing events are reported with an uncertainty corresponding to one event. This uncertainty is not added to the total MC contribution. Systematic uncertainties (the second uncertainty if present) are displayed only for the final combined type of background, no systematic uncertainty is added for estimates with zero entries. Systematic uncertainties are 100% correlated among the channels.

The estimation is in a good agreement with the observation. We also note that the backgrounds with respect to the inclusive same-sign dilepton search is suppressed by an order of magnitude due to the b-tag requirements. As seen in the yield tables above, the contribution from fake leptons from b-quark decays in $t\bar{t}$, which is the dominant in the pre-tagged sample analysis [3], is now suppressed and is no longer a dominant one. This confirms our initial expectation from requiring two b-tagged jets.

This section is missing two things. First, we will add a $\not\!\!E_T$ vs H_T plot that shows the data and one of the models overlayed. Second, we will add a summary of the events we see.

9 Acceptance Systematics

Systematic uncertainties on signal event selections arise from uncertainties on event selections expected in simulation compared to the actual performance of the detector. The uncertainties associated with the data - Monte Carlo scale factors are discussed in Section 5 As this search is in many ways similar to the inclusive same-sign dilepton search [3], our treatment of efficiency systematics parallels the one in that analysis. In this section, we briefly summarize those results, and describe the uncertainties due to the b-tagging requirement.

The only new source of systematics in this analysis is from the uncertainty on the b-jet tagging efficiency. As already mentioned in Section 5.2, this uncertainty is 4 (15)% for jets with $p_T < 240 (> 240)$ GeV. As an illustration of the b-jet momentum distribution, we compare them in Fig. 8 for $t\bar{t}$ events (before the same-sign requirement) and for the LM9 cMSSM SUSY benchmark point.[3)] While most of the b-jets from $t\bar{t}$ are below 240 GeV, those from LM9 have a large contribution from higher momenta. Our target searches include final states with two or more b-quark jets. This means the efficiency to select two b-jets, as well as its uncertainty varies among the signal final states considered

- same-sign top pair production, as from Z' exchange, is similar in topology to that of the opposite-sign $t\bar{t}$ production and has only two b-jets in the final state with most of them with $p_T < 240$ GeV. The b-tagging uncertainty is then approximately 8% and the corresponding per-event scale factor is 0.922 ± 0.073.
- direct sbottom pair production has two b-jets in the final state with a large fraction of b-jets with $p_T >$ 240 GeV. The b-tagging efficiency scale factor is still 0.922, but its uncertainty varies among the signal model points from as low as 8% to as high as 29%. This uncertainty is evaluated event-by-event and then point-by-point in the limit setting procedure.
- gluino pair production with stops in the final states considered here all have four b-jets in the final state. Now the efficiency scale factor changes as well depending on the number of b-jets in the acceptance. This is evaluated event-by-event and point-by point in the limit setting procedure.

A summary of systematic uncertainties is given in Table 17. Here the b-tagging systematics is applicable only to the same-sign top production signature.

Table 17: Summary of systematic uncertainties on the signal selection and expectation. Reported values are fractional, relative to the total cross section. The energy scale, b-tagging, and PDF uncertainties are calculated separately in every model point. These uncertainties quoted here are relevant to the Z' model.

Source	ee	$\mu\mu$	$e\mu$	all
Lepton selection	12%	12%	11%	11%
Energy scale	8%	8%	8%	8%
ISR/FSR and PDF	2%	2%	2%	2%
b-tag selection	8%	8%	8%	8%
Total without luminosity	17%	17%	17%	17%
Integrated luminosity	4.5%	4.5%	4.5%	4.5%
Total	17%	17%	17%	17%

[3)] The LM9 point is defined by the common scalar mass (m0) $= 1.45$ TeV, the common gaugino mass (m1/2) = 175 GeV, the ratio of the Higgs expectation values (tan$\beta) = 10$, tri-linear coupling (A0) = 0 and the sign of the Higgsino mass parameter $(\mu) > 0$.

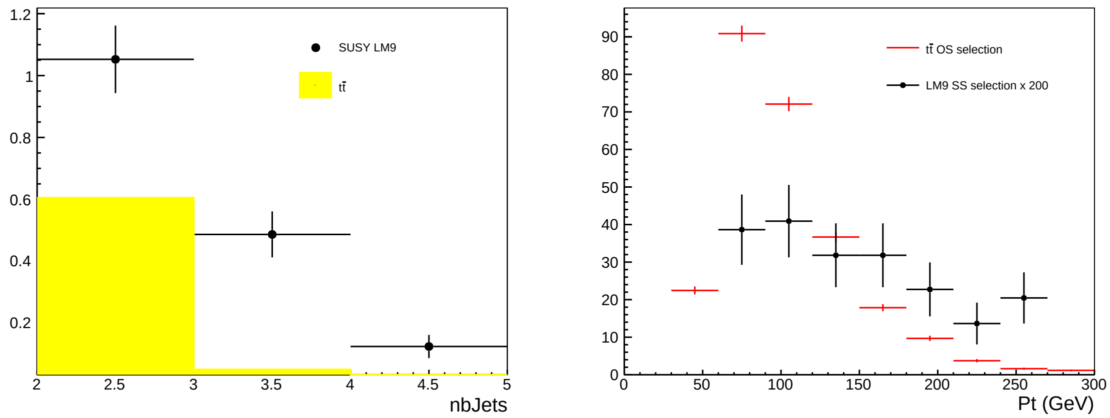

Figure 8: Differential distributions of leading b-tag jet p_T for the LM9 benchmark point and $t\bar{t}$ simulations. The normalization is arbitraty.

9.1 Event-by-Event B-tagging scale factor and associated systematic uncertainty

We evaluate an event-by-event btagging scale factor (SF_{event}) as follows:

- for each MC event passing the event selection we start from the scale factors SF_i associated with the two or more tagged jets. Note that SF_i can in principle be a function of jet η, p_T, etc. Following the btag group recommendations it is taken as a constant: $SF = 0.96$[5, 35].
- For events with two btagged jets: $SF_{\text{event}} = SF^2$.
- For events with three btagged jets: $SF_{\text{event}} = SF^3 + 3SF^2(1 - SF)$.
- For events with four btagged jets: $SF_{\text{event}} = SF^4 + 4SF^3(1 - SF) + 6SF^2(1 - SF)^2$.

Note that the procedure above would not work if $SF > 1$, but this is not an issue since $SF = 0.96$. It also implicitely assumes that all btags are from b-quarks. For the models under consideration, we have verified that the MC contribution to the acceptance from events that need at least one tag from $udsgc$ in order to pass the ≥ 2 tags requirements is small. For example, in the Z' model, this contribution is only $\approx 4\%$. Note that the bias in SF_{event} due to the improper traeatment these events is 4% times some quantity proportional to the difference in scale factors between b-jets and $usdgc$ jets. Therefore, it is $<< 4\%$ and we think can be ignored.

In order to calculate the uncertainty (δSF) on the event-by-event SF_{total}, we also need the single jet btagging efficiency (ϵ). We do not need a very precise value for ϵ, since the uncertainty δSF is only weakly dependent on it. We take $\epsilon = 0.643$, independent of p_T and η for jets of $|\eta| < 2.5$. The uncertainty on ϵ is the same as that on the scale factors, $\delta\epsilon = 4\%(15\%)$ (relative) for $p_T < 240$ GeV (> 240 GeV). The procedure is the following:

- For each event passing the requirements at RECO level, we look at the status=3 information and we calculate the total probability (p) of tagging two or more jets, and its uncertainty (δp).
- The calculation of p and δp is based on the number of status=3 b-quarks of $p_T > 40$ GeV and $|\eta| < 2.5$.
- An event with two reconstructed btags can have < 2 such status=3 b-quarks. This is rare and happens for example when a 39 GeV b-quark is reconstructed as a 41 GeV b-jet. In these cases we calculate p and δp assuming that there are two 40 GeV b-quarks at status=3.
- The uncertainty associated with the event is then $(\frac{|\delta p|}{p})SF_{\text{event}}$.

The probabilities p are calculated as follows (N here is the number of status=3 b-quarks and we write the equations without the assumtion that ϵ is constant):

- $N = 2$: $\quad p = \epsilon_1\epsilon_2$.
- $N = 3$: $\quad p = \epsilon_1\epsilon_2 + \epsilon_1\epsilon_3 + \epsilon_2\epsilon_3 - 2\epsilon_1\epsilon_2\epsilon_3$.

- $N = 4$:

$$p = \prod \epsilon_i \quad + \quad \sum_j (1-\epsilon_j) \prod_{i \neq j} \epsilon_i \quad + \quad \sum_{j<k} (1-\epsilon_j)(1-\epsilon_k) \prod_{i \neq j,k} \epsilon_i$$

The uncertainties δp are calculated from the equations above assuming full correlation between jets, *e.g.*, for $N = 2$ we have $\delta p = \delta\epsilon_1 \cdot \epsilon_2 + \delta\epsilon_2 \cdot \epsilon_1$, etc.

10 Searches for Specific Models

Our signature, two isolated same-sign leptons plus, at least two b-tagged jets, and $\not\!\!E_T$, is common to many different new physics scenarios. Here we refine our analysis to define dedicated signal regions for a few of these scenarios, and provide 95% C.L. upper limits on their respective model parameter space.

10.1 Same sign top production due a Z'

This is an extension of the 2010 CMS published CMS analysis[1]. The main difference is that here in order to improve the signal-to-noise we require two b-tagged jets. This would not have made sense in 2010, since at the time the integrated luminosity was low enough that the analysis was almost background free without requiring b-tags.

10.1.1 Theoretical Discussion, Z' model

Recent measurements of the inclusive forward-backward $t\bar{t}$ production asymmetry (A_{FB}) from the Tevatron experiments show deviations from the standard model (SM) expectations [36, 37, 38]. Several attempts have been made to explain this asymmetry [39, 40, 41, 42]. One of the most natural ways to induce such an asymmetry would be through Flavor Changing Neutral Currents (FCNC) in the top quark sector. The forward-backward asymmetry in $u\bar{u} \to t\bar{t}$ would then be generated by t-channel exchange of a new massive Z' boson that couples chirally to u and t at the same vertex, as shown in Fig. 9 [39]. The same type of interaction would also give rise to same-sign top pair production, as illustrated in Fig. 10 and Fig. 11. In this case, the initial state involves two $u-$quarks and thus the cross section at the LHC is enhanced due to the large valence quark parton density of the proton.

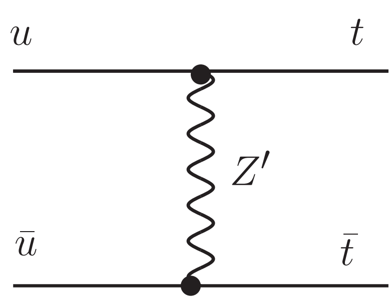

Figure 9: Diagram for $t\bar{t}$ production induced by Z' exchange which can generate a forward-backward asymmetry.

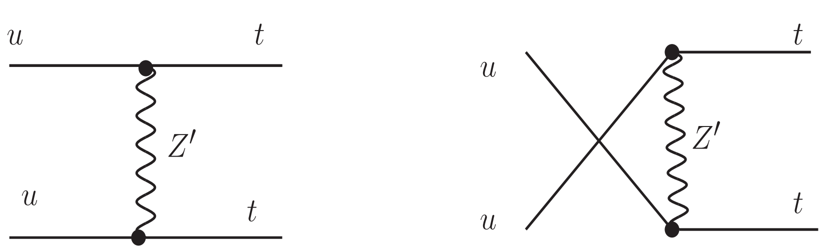

Figure 10: Diagrams for tt pair production induced by Z' exchange in the t-channel.

We consider the model of Reference [39]. The relevant $u - t - Z'$ interaction term in the Lagrangian is:

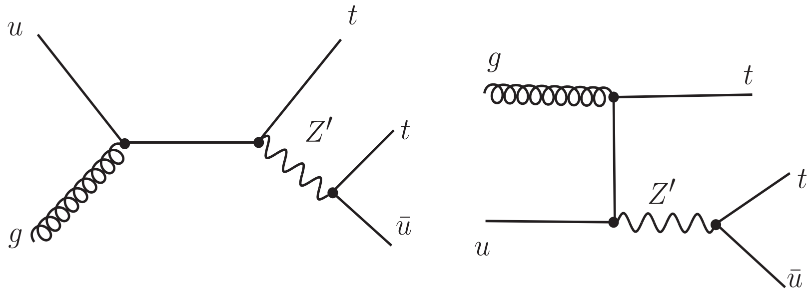

Figure 11: Diagrams for $tt\bar{u}$ production induced by Z' exchange in the s-channel

$$\mathcal{L} = g_W \bar{u}\gamma^{\mu}(f_L P_L + f_R P_R)tZ'_{\mu} + h.c \tag{2}$$

where g_W is the weak coupling strength. The left-handed coupling is set to $f_L = 0$, due to the $B_d - \bar{B}_d$ mixing constraint [45]. The right-handed coupling f_R and the Z' mass are free parameters in the model. Within this model there is a narrow range of parameter space consistent with the TeVatron measurements of $\sigma(p\bar{p} \to t\bar{t})$ and A_{FB}, which is not excluded by direct searches for same sign tops. This region is illustrated in Fig. 12.

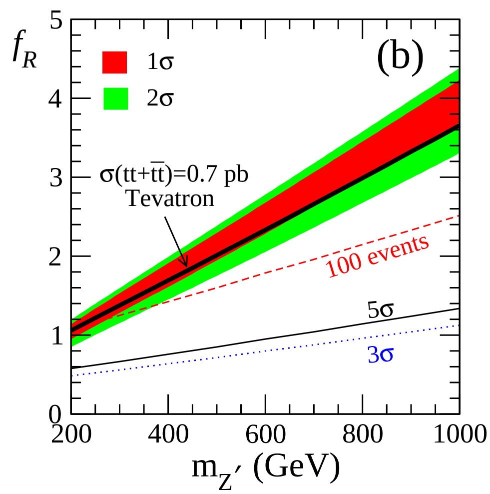

Figure 12: From Reference [39]; the shaded area covers the parameter space consistent with the A_{FB} and $\sigma(t\bar{t})$ from the Tevatron; The line indicated by the arrow shows the Tevatron limit inferred by the authors from same sign top searches at the Tevatron; the remaining lines represent the expectations of Reference [39] for LHC searches in 1 fb^{-1}.

Monte Carlo events for this model were generated using Madgraph in the same way as for the 2010 analysis (see Reference [48]).

10.1.2 Signal region definition for same sign top from Z'

In this study we search for same-sign dileptons originating from tt or ttj pair production as described above. At the LHC $uu \to tt$ dominates over $\bar{u}\bar{u} \to \bar{t}\bar{t}$, thus we concentrate on same-sign positive leptons. The $\not{E}_T$ and H_T cuts are typical of a dilepton top analysis: two or more jets of $P_T > 40$ GeV, $\not{E}_T > 30$ GeV and $H_T > 80$ GeV. This corresponds to Table 11: 5 events observed and $4.42 \pm 0.80 \pm 1.39$ expected from background.

10.1.3 Limits on the Z' model

Using the results from Section 10.1.2, we set a limit at 95% CL of 7.2 events using the CL$_\text{S}$ method. The expected limit is 6.4 events. In the MC we find $Acc \times Eff \times BR = 0.00233$, independent of Z' mass. This results in an upper limit on the cross-section of 0.67 pb. The limit includes uncertainty on JES (12%), btagging (10%), lepton efficiencies (11%), luminosity (4.5%), and PDF (3%).

The cross-section limit is turned into an exclusion limit in the $m(Z')$ vs f_R plane using the LO calculation of the $pp \rightarrow tt$ cross-section in this model. This is shown in Figure 13, together with the corresponding plot from the 2010 analysis.

For $M_{Z'} >> M_{\rm top}$ the Lagrangian of equation 1 is equivalent to $\mathcal{L} = -\frac{1}{2}\frac{C_{RR}}{\Lambda^2}[\bar{u}\gamma^{\mu}t][\bar{u}\gamma_{\mu}t] + h.c.$ [46], with $\frac{C_{RR}}{\Lambda^2} = \frac{2g_W^2 f_R^2}{M_{Z'}^2}$. Our limit on f_R, calculated for $M_{Z'} = 2$ TeV, would then correspond to $\frac{C_{RR}}{\Lambda^2} < 0.6$ TeV^{-2} at 95% confidence. This is more stringent than the limit recently reported by CDF: $\frac{C_{RR}}{\Lambda^2} < 3.7$ TeV^{-2} [47].

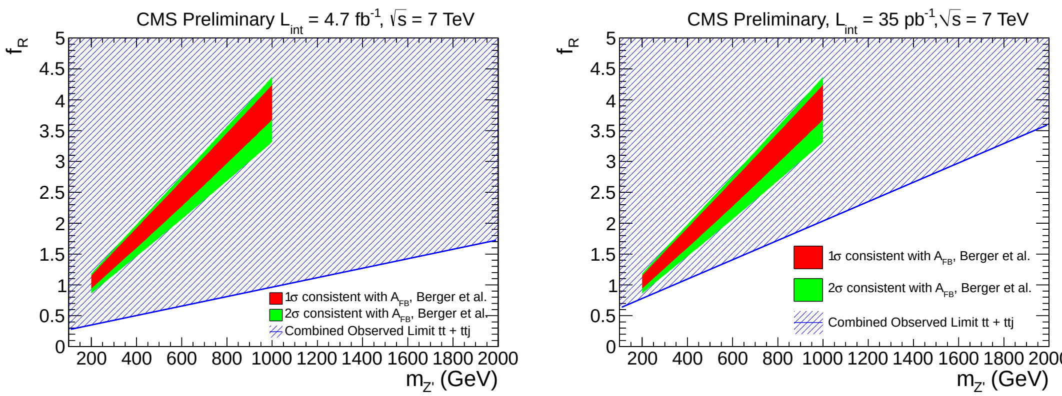

Figure 13: Exclusion regions from the 2011 analysis (left) and the 2010 analysis (right). The exclusions are obtained using the LO cross-section for tt production. Note that the cross-section is proportional to f_R^4.

10.1.4 What is still missing for the Z' model

- Double check calculation of $\frac{C_{RR}}{\Lambda^2}$
- Double check acceptance numbers

10.2 Maximally Flavor Violation Model (MXFV)

10.2.1 Theoretical discussion of MXFV

This is a model [26, 27, 28] with a new scalar SU(2) doublet field $\Phi_{FV} = (\eta^0, \eta^+)$ that couples the first and third generation quarks (q_1, q_3) via a Lagrangian term $\mathcal{L}_{FV} = \xi_{13}\Phi_{FV} q_1 q_3$. Remarkably, it appears that this model is largely consistent with constraints from flavor physics.

The model results in same sign top pairs in the final state as foolows

- Single η^0 production: $ug \to t\eta^0 \to tt\bar{u}, t\bar{t}u$
- η^0 pair production: $u\bar{u} \to \eta^0\eta^0 \to tt\bar{u}\bar{u}, uu\overline{tt}, t\bar{t}u\bar{u}$
- η^0 t-channel exchange: $uu \to tt$, $\bar{u}\bar{u} \to \overline{tt}$

Monte Carlo events were generated using LHE files[13] interfaced with Madgraph. Madgraph was used to decay the top quarks in order to preserve spin-correlations. The cross-sections at LO for same sign tt pairs for the three processes in the MXFV model is shown in Figure 14. The t-channel process is the most important.

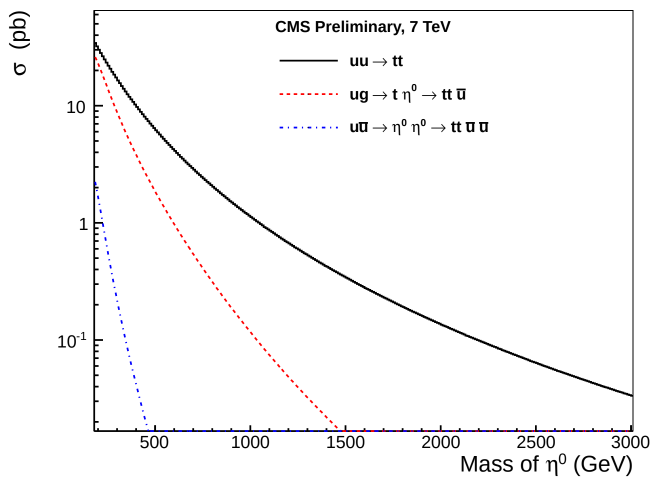

Figure 14: Cross section at LO for the tt final state in the three MXFV modes as a function of η^0 mass for $\xi = 1$.

10.2.2 Signal region definition for the MXFV model

The properties of the final state in this model are basically the same as in the Z' model. Thus, we use the same signal region definition (see Section 10.1.2).

10.2.3 Limits for the MXFV model

Our limits in the ξ-M(η^0) plane are shown in Figure 15. They are calculated using the LO cross-section for this model.

10.2.4 What is still missing for the MXFV model

- Need to include the $tt\bar{u}$ final state
- Rescale everything to take into account that the leptonic BR in MG is not quite right
- Signal Contamination effects (should be tiny)
- Prettify the exclusion plot, put CDF on same plot perhaps

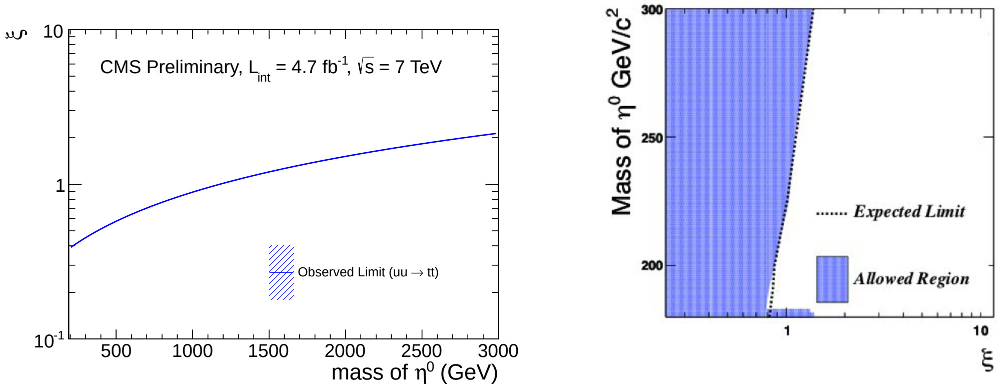

Figure 15: Limits in the ξ-Mass(χ^0) plane. Left: CMS. Right: CDF

10.3 $\widetilde{g} \to t\widetilde{t}$ Model

10.3.1 Theoretical discussion of the $\widetilde{g} \to t\widetilde{t}$ Model

This is an interesting model for stop pair production through gluino decays[9][10][23][19]. It is a "realistic" and well-motivated model in the sense that it applies to the situation where all the squarks except the stop are very heavy. A "light" stop is of course generally favored in SUSY, and LHC results are pointing to "heavy" superpartners. Then if the stop is light enough the gluino would decay with 100% BR as $\widetilde{g} \to t\widetilde{t}$ and then the stop would decay as $\widetilde{t} \to t\chi_1^0$, if kinematically accessible. The parameters of the model are $M(\widetilde{g})$, $M(\widetilde{t})$, $M(\chi_1^0)$.

The final state after gluino pair production is then $tt\overline{t}\overline{t}\chi_1^0\chi_1^0$. It is the same final state as the `T1tttt` **(need a reference here)** simplified model, except that it proceeds through an intermediate stop. This final state is rich in leptons, and has four b-quarks. The same sign dilepton + btags + $\not{E}_T$ signature is a particularly good way to go after it.

10.3.2 Signal region definition for the $\widetilde{g} \to t\widetilde{t}$ Model

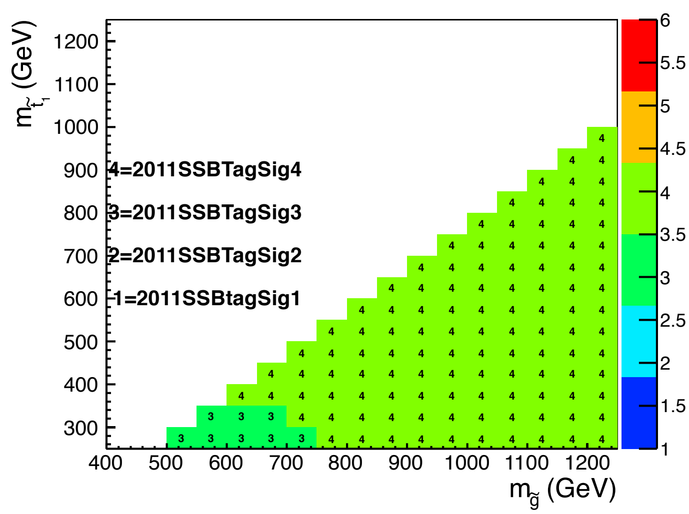

Figure 16: The signal region with the best expected limit as a function of $m(\widetilde{g}$ vs. $m(\widetilde{t})$ plane for $m(\chi_1^0)$=50 GeV. The coding is: 1=(200-50), 2=(200-150), 3=(320-50), and 4=(320-120), where the first (second) number is the H_T ($\not{E}_T$) threshold in GeV.

For each point in parameter space we use the signal region that gives the best expected limit. Limits are calculated using all experimental uncertainties; the JES and btag uncertainties are calculated point-by-point. An example of this optimization is shown in Figure 16, where we show the choice of signal region that gives the best expected limit in the $m(\widetilde{g}$ vs. $m(\widetilde{t})$ plane for the choice $m(\chi_1^0)$=50 GeV.

10.3.3 Limits for the $\widetilde{g} \to t\widetilde{t}$ Model

The limits on the production cross-section in this model in the gluino mass vs. stop mass plane for two choices of the LSP mass are shown in Figure 17 Using the NLO+NLL cross-section for gluino pair production, we als place a limit on the mass parameters of this model.

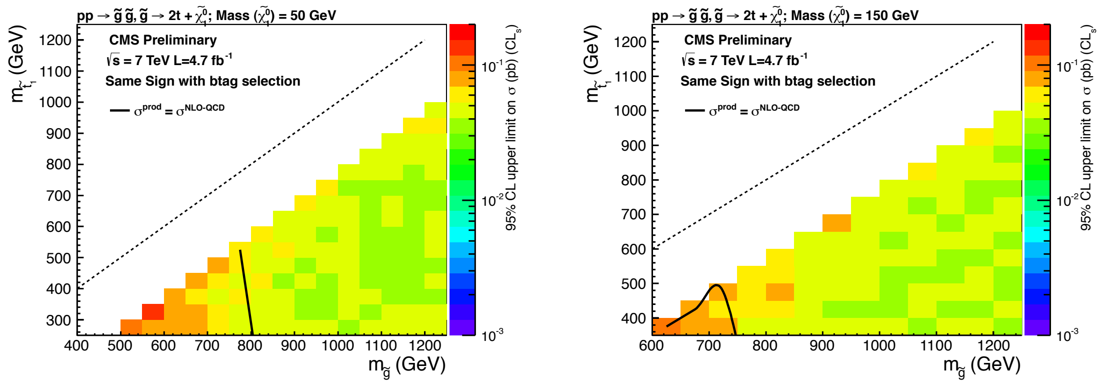

Figure 17: Cross section limits in the $m(\widetilde{g})$ vs. $m(\widetilde{t})$ plane for $m(\chi_1^0)$ = 50 GeV (left) and 150 GeV (right).

10.3.4 What is missing for the $\widetilde{g} \to t\widetilde{t}$ Model

- Perhaps more details on the MC signal generation???
- Need a reference for the `T1tttt` model
- Maybe also a plot for LSP mass = 100 GeV?

10.4 `T1tttt` Model

10.4.1 Theoretical discussion of the `T1tttt` Model

The `T1tttt` **(need a reference)** simplified model is very similar to the model of Section 10.3. In this model it is assumed that all squarks are very heavy, but the stop is somewhat lighter than the other quarks[20][21]. Then the gluino would decay as $\widetilde{g} \to t\bar{t}\chi_1^0$ through virtual stops. Other gluino decay modes would be suppressed because the stop is the lightest squark. The final state after gluino pair production is $tt\bar{t}\bar{t}\chi_1^0\chi_1^0$, just as in Section 10.3. The model parameters are $M(\widetilde{g})$ and $M(\chi_1^0)$.

10.4.2 Signal region definition for the `T1tttt` Model

For each point in parameter space we use the signal region that gives the best expected limit. The limits include all experimental uncertainties. The JES and btag uncertainties are calculated point-by-point.

10.4.3 Limits for the `T1tttt` Model

The limit on the production cross-section in this model in the gluino mass vs. LSP mass plane shown in Figure 18. Using the NLO+NLL cross-section for gluino pair production, we place a limit on the mass parameters as shown in Figure 18.

10.4.4 What is missing for the `T1tttt` Model

- Need at least a sentence to say something which signal region contributes. Or a plot.
- Need a reference for the `T1tttt` model

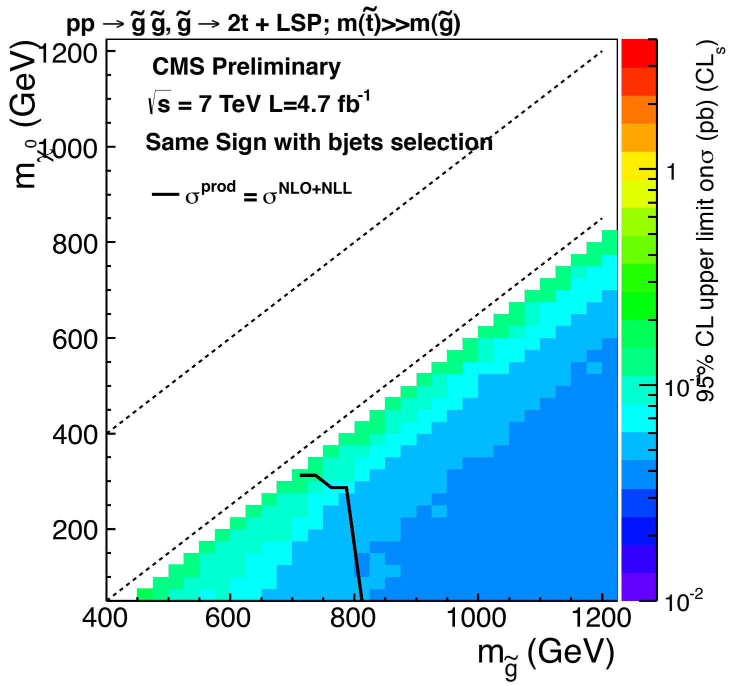

Figure 18: Cross section limits in the $m(\widetilde{g})$ vs. $m(\chi_1^0)$ plane for the `T1tttt` model.

10.5 Sbottom pair production Model

In this model we have $pp \to \tilde{b}\tilde{\bar{b}}$. The sbottom decays as $\tilde{b} \to t\chi^-$ followed by $\chi^- \to W^-\chi_1^0$. The final state is $t\bar{t}W^+W^-\chi_1^0\chi_1^0$. The model parameters are $M(\widetilde{b})$, $M(\chi_1^0)$, and $M(\chi^\pm)$. For simplicity we only consider mass parameters such that the χ^- is on shell.

10.5.1 Signal region definition for the sbottom pair production model

For each point in parameter space we will use the signal region that gives the best expected limit.

10.5.2 Limits for the sbottom pair production model

Nothing yet. The money plot will be exclusion lines in the 2D plot of sbottom mass vs. LSP mass for a few choices of the $\chi^\pm$ mass.

10.5.3 What is missing for the sbottom pair production model

- Everything in Sections 10.5.1 and 10.5.2
- It would be nice to have a reference. I am not sure that the references that we have on our twiki are appropriate.
- Perhaps more details on the MC signal generation

10.6 $\widetilde{g} \to \widetilde{b}\bar{b}$ Model

This model is mostly gluino pair production followed by $\widetilde{g} \to \widetilde{b}\bar{b}$, $\widetilde{b} \to t\chi^-$ and $\chi^- \to W^-\chi_1^0$. The final state is $t\bar{t}b\bar{b}W^+W^-\chi_1^0\chi_1^0$ or $ttb\bar{b}W^+W^-\chi_1^0\chi_1^0$ $(+c.c.)$. The model also includes the $bg \to \widetilde{b}\widetilde{g}$ process, in which case the final state is $tb\bar{b}W^+W^-\chi_1^0\chi_1^0$ $(+c.c.)$. The model parameters are $M(\widetilde{g})$ $M(\widetilde{b})$, $M(\chi_1^0)$, and $M(\chi^\pm)$. For simplicity we only consider mass parameters such that the χ^- is on shell.

10.6.1 Signal region definition for the $\widetilde{g} \to \widetilde{b}\overline{b}$ Model

For each point in parameter space we will use the signal region that gives the best expected limit.

10.6.2 Limits for the $\widetilde{g} \to \widetilde{b}\overline{b}$ Model

Nothing yet. The money plot will be exclusion lines in the 2D plot of gluino mass vs. sbottom mass for a few choices of the $\chi^{\pm}$ and χ_1^0 masses.

10.6.3 What is missing for the $\widetilde{g} \to \widetilde{b}\overline{b}$ Model

- Everything in Sections 10.6.1 and 10.6.2
- It would be nice to have a reference. I am not sure that the references that we have on our twiki are appropriate.
- Perhaps more details on the MC signal generation

11 Outreach

As mentioned in Section 4, we want to provide enough information so that anybody can use their favorite Monte Carlo generator of new physics, define an acceptance at the hard scatter level (status = 3 in Pythia), and correctly estimate the efficiency for this new physics model to within 50% or so.

The relevant information on selection efficiencies is given in Section 4. In this Section we give the missing ingredients for this program, namely the 95% upper limits on the number of events for the various signal regions. We also show how well our efficiency model works in a few cases.

11.1 Limits on number of events

Here we should give the limits on the number of events for the various signal region definitions. This is always a little tricky because we always debate what uncertainties to include. I guess we came up with a receipe in the generic analysis (both 2010 and 2011), but I don't remember what waht we did. In any case, we should do the same here and describe it. It should take $<$ 1 hour. What we want is a Table with concise signal region definition, number of observed events, total BG, and UL on new physics contribution expressed in number of events.

11.2 Testing the efficiency model

We should take two or three model-points and compare the efficiency times acceptance for the simulation and the efficiency model. This is a little bit of work (maybe one day's worth?)

12 Conclusion

In conclusion, the first search using same-sign dileptons with b-jets and $\not\!\!E_T$ has been presented. In the proton-proton collision data sample corresponding to an integrated luminosity of 4.7 fb^{-1} at $\sqrt{s}$ = 7 TeV, no significant deviations from the Standard Model expectations are observed. We use this data to set 95% CL. on the number of observed events. We set limits on the parameter space of six new physics models:

1. A model with a Z' vector boson with flavor violating couplings to $u-$ and t-quarks.
2. A model with a neutral scalar with flavor violating couplings to $u-$ and t-quarks.
3. A SUSY model of stop production from two body gluino decays: $pp \to \widetilde{g}\widetilde{g}$ followed by $\widetilde{g} \to t\widetilde{t}$ and $\widetilde{t} \to t\chi_1^0$.
4. A SUSY model of stop pair production from three body gluino decays: $pp \to \widetilde{g}\widetilde{g}$ followed by $\widetilde{g} \to t\widetilde{t}\chi_1^0$.
5. A SUSY model of sbottom pair production: $pp \to \tilde{b}\bar{\tilde{b}}$ followed by $\tilde{b} \to t\chi^-$ and $\chi^- \to W^-\chi_1^0$.
6. A SUSY model of sbottom production from gluino decays: $pp \to \widetilde{g}\widetilde{g}$ followed by $\widetilde{g} \to \widetilde{b}\overline{b}$, $\widetilde{b} \to t\chi^-$, and $\chi^- \to W^-\chi_1^0$.

Finally, we provide enough experimental information to allow interested phenomenologists to use our data to confront additional new physics models in an approximate way.

We need to prune this list of obsolete stuff, improve the level of detail in some cases (missing titles, etc), and put the reference in the right order. Lots of tedious work...

References

[1] S. Chatrchyan *et al.* [CMS Collaboration], *"Search for Same-Sign Top-Quark Pair Production at $\sqrt{s}$ = 7 TeV and Limits on Flavour Changing Neutral Currents in the Top Sector,"* JHEP **1108**, 005 (2011) [arXiv:1106.2142 [hep-ex]].

[2] S. Chatrchyan *et al.* [CMS Collaboration], *"Search for new physics with same-sign isolated dilepton events with jets and missing transverse energy at the LHC,"* JHEP **1106**, 077 (2011) [arXiv:1104.3168 [hep-ex]].

[3] *"Search for New Physics with Same-Sign dileptons using the 2011 dataset of CMS"*, CMS AN-2011/468.

[4] CMS Collaboration, *"Search for new physics with same-sign isolated dilepton events with jets and missing energy"*, CMS PAS SUS-11-010/SUS-11-025, in preparation.

[5] CMS Collaboration, *"Measurement from data of efficiency and mistag rate of b-tagging algorithms using 2010 data"*, PAS BTV-11-001 (Submitted)

[6] *"Fake Rates for Dilepton Analyses"*, CMS AN-2010/257.

[7] A.L. Read, CERN Report 2000-005 p. 81 (2000).

[8] whatever, some bayesian reference.

[9] http://arxiv.org/abs/hep-ph/0512284,SUSY Gluinos to light stop

[10] http://arxiv.org/abs/1004.2256,more SUSY Gluinos to light stop

[11] The same sign top, E. Berger et al.

[12] http://arxiv.org/abs/0801.1679, $T_{5/3}$ fermion pair production leading to $t\bar{t}W^+W^-$ final state.

[13] http://lhcnewphysics.org/l.006.00.r000, Simplified model by Felix Yu, UCI

[14] http://lhcnewphysics.org/b.011.00.r000 , Stop anti-stop production proposal by Toro et al.

[15] http://lhcnewphysics.org/b.007.00.r000 , $t\bar{t}t\bar{t}$ production via pair production of a neutral color octet resonance by Toro et al.

[16] A. G. Cohen, D. B. Kaplan and A. E. Nelson, *"The More minimal supersymmetric standard model,"* Phys. Lett. B **388**, 588 (1996) [hep-ph/9607394].

[17] S. Dimopoulos and G. F. Giudice, *"Naturalness constraints in supersymmetric theories with nonuniversal soft terms,"* Phys. Lett. B **357**, 573 (1995) [hep-ph/9507282].

[18] R. Barbieri, G. R. Dvali and L. J. Hall, *"Predictions from a U(2) flavor symmetry in supersymmetric theories,"* Phys. Lett. B **377**, 76 (1996) [hep-ph/9512388].

[19] M. Papucci, J. T. Ruderman and A. Weiler, *"Natural SUSY Endures,"* arXiv:1110.6926 [hep-ph].

[20] B. S. Acharya, P. Grajek, G. L. Kane, E. Kuflik, K. Suruliz and L. -T. Wang, *"Identifying Multi-Top Events from Gluino Decay at the LHC,"* arXiv:0901.3367 [hep-ph].

[21] G. L. Kane, E. Kuflik, R. Lu and L. -T. Wang, *"Top Channel for Early SUSY Discovery at the LHC,"* Phys. Rev. D **84**, 095004 (2011) [arXiv:1101.1963 [hep-ph]].

[22] S. Kraml and A. R. Raklev, *"Same-sign top quarks as signature of light stops at the LHC,"* Phys. Rev. D **73**, 075002 (2006) [hep-ph/0512284].

[23] R. Essig, E. Izaguirre, J. Kaplan and J. G. Wacker, *"Heavy Flavor Simplified Models at the LHC,"* arXiv:1110.6443 [hep-ph].

[24] T. Plehn and T. M. P. Tait, *"Seeking Sgluons,"* J. Phys. G G **36**, 075001 (2009) [arXiv:0810.3919 [hep-ph]].

[25] M. Gerbush, T. J. Khoo, D. J. Phalen, A. Pierce and D. Tucker-Smith, *"Color-octet scalars at the CERN LHC,"* Phys. Rev. D **77**, 095003 (2008) [arXiv:0710.3133 [hep-ph]].

[26] S. Bar-Shalom and A. Rajaraman, *"Models and phenomenology of maximal flavor violation,"* Phys. Rev. D **77**, 095011 (2008) [arXiv:0711.3193 [hep-ph]].

[27] S. Bar-Shalom, A. Rajaraman, D. Whiteson and F. Yu, *"Collider Signals of Maximal Flavor Violation: Same-Sign Leptons from Same-Sign Tops at the Tevatron,"* Phys. Rev. D **78**, 033003 (2008) [arXiv:0803.3795 [hep-ph]].

[28] T. Aaltonen *et al.* [CDF Collaboration], *"Search for Maximal Flavor Violating Scalars in Same-Charge Lepton Pairs in $p\bar{p}$ Collisions at $\sqrt{s}$ = 1.96-TeV,"* Phys. Rev. Lett. **102**, 041801 (2009) [arXiv:0809.4903 [hep-ex]].

[29] R. Contino and G. Servant, *"Discovering the top partners at the LHC using same-sign dilepton final states,"* JHEP **0806**, 026 (2008) [arXiv:0801.1679 [hep-ph]].

[30] B. Lillie, J. Shu and T. M. P. Tait, *"Top Compositeness at the Tevatron and LHC,"* JHEP **0804**, 087 (2008) [arXiv:0712.3057 [hep-ph]].

[31] A. Pomarol and J. Serra, *"Top Quark Compositeness: Feasibility and Implications,"* Phys. Rev. D **78**, 074026 (2008) [arXiv:0806.3247 [hep-ph]].

[32] K. Kumar, T. M. P. Tait and R. Vega-Morales, *"Manifestations of Top Compositeness at Colliders,"* JHEP **0905**, 022 (2009) [arXiv:0901.3808 [hep-ph]].

[33] E. L. Berger, Q. -H. Cao, C. -R. Chen, C. S. Li and H. Zhang, *"Top Quark Forward-Backward Asymmetry and Same-Sign Top Quark Pairs,"* Phys. Rev. Lett. **106**, 201801 (2011) [arXiv:1101.5625 [hep-ph]].

[34] CMS Collaboration, *"Measurement of the b-tagging efficiency using $t\bar{t}$ events"*, PAS BTV-11-003, in preparation.

[35] M. Narain for BTV POG, `https://indico.cern.ch/getFile.py/access?contribId=0&resId=1&materialId=slides&confId=163892`

[36] D0 Collaboration, "First measurement of the forward-backward charge asymmetry in top quark pair production", Phys.Rev.Lett.100:142002, (2008)

[37] CDF Collaboration, "Forward-Backward Asymmetry in Top Quark Production in $p\bar{p}$ Collisions at $sqrts =$ 1.96 TeV", Phys.Rev.Lett.101:202001, (2008)

[38] CDF Collaboration, "Evidence for a Mass Dependent Forward-Backward Asymmetry in Top Quark Pair Production", arXiv:1101.0034, (2011)

[39] Ed.Berger et. al, "Top Quark Forward-Backward Asymmetry and Same-Sign Top Quark Pairs", arXiv:1101.5625, (2011)

[40] M.R. Buckley et. al, "Light Z' Bosons at the Tevatron", arXiv:1103.6035, (2011)

[41] Moira I. Gresham et. al, "On Models of New Physics for the Tevatron Top AFB", arXiv:1103.3501, (2011)

[42] Z.Ligeti et. al, "Explaining the t tbar forward-backward asymmetry without dijet or flavor anomalies", arXiv:1103.2757, (2011)

[43] C.T Hill, Phys. Lett. B345, 483 (1995)

[44] R.S. Chivukula, E.H. Simmons and J. Terning, Phys.Lett.B331,383 (1984); D.J. Muller and S. Nandi, Phys.Lett.B383,345 (1996); E. Malkawi, T. Tait and C.-P. Yuan, Phys.Lett.B385,304 (1996); K. Lane and E.Eichten, Phys.Lett.B433,96 (1998); C.T. Hill, Phys.Rev.D59,075003 (1999); H. Georgi and A.K. Grant, Phys.Rev.D63,015001 (2001).

[45] Q.H. Cao et. al. Phys.Rev.D81, 114004 (2010)

[46] J. A. Aguilar-Saavedra, "Effective four-fermion operators in top physics: a roadmap", Nucl. Phys. B843 (2011), arXiv:1008:3562.

[47] "Search for like-sign top quark pair production at CDF with 6.1 fb^{-1}", CDF/PHYS/EXO/PUBLIC/10466, http://www-cdf.fnal.gov/physics/exotic/r2a/20110407.samesigndileptons/sstops.pdf

[48] CMS AN-2011/137

A Results - Exclusive Yields

The tighter H_T and $\not\!\!E_T$ search regions used for the SUSY production scenarios and defined in Section 3 can be defined exclusively and cover the same phase space without an overlap between regions:

1. Exclusive low-H_T low-$\not\!\!E_T$ region: $200 < H_T < 320$ GeV, $50 < \not\!\!E_T < 120$ GeV.
2. Exclusive low-H_T high-$\not\!\!E_T$ region: $200 < H_T < 320$ GeV, $\not\!\!E_T > 120$ GeV.
3. Exclusive high-H_T low-$\not\!\!E_T$ region: $H_T > 320$ GeV, $50 < \not\!\!E_T < 120$ GeV.
4. Exclusive high-H_T high-$\not\!\!E_T$ region: $H_T > 320$ GeV, $\not\!\!E_T > 120$ GeV.

The exclusive high-H_T high-$\not\!\!E_T$ region is the same as its inclusive version.

In the following we report exclusive breakdown of the expected and observed events in the H_T-$\not\!\!E_T$ SUSY search regions. These are reported in Tables 18 to 20. The formatting of these tables is the same as in Section 8. Results for the exclusive high-H_T high-$\not\!\!E_T$ region are not repeated and can be found in Table 15.

Source	ee	$\mu\mu$	eμ	all
$t\bar{t} \to \ell\ell X$	0.017 $\pm$ 0.199	0.000 $\pm$ 0.199	0.000 $\pm$ 0.199	0.017 $\pm$ 0.199
$t\bar{t}$ other	0.000 $\pm$ 0.199	0.000 $\pm$ 0.199	0.000 $\pm$ 0.199	0.000 $\pm$ 0.199
$t\bar{t} \to \ell(b \to \ell)X$	0.000 $\pm$ 0.199	0.000 $\pm$ 0.199	0.000 $\pm$ 0.199	0.000 $\pm$ 0.199
$t\bar{t} \to \ell(\not{b} \to \ell)X$	0.026 $\pm$ 0.199	0.000 $\pm$ 0.199	0.049 $\pm$ 0.199	0.075 $\pm$ 0.199
t, s-channel	0.000 $\pm$ 0.057	0.000 $\pm$ 0.057	0.000 $\pm$ 0.057	0.000 $\pm$ 0.057
t, t-channel	0.000 $\pm$ 0.055	0.000 $\pm$ 0.055	0.000 $\pm$ 0.055	0.000 $\pm$ 0.055
tW	0.000 $\pm$ 0.045	0.000 $\pm$ 0.045	0.000 $\pm$ 0.045	0.000 $\pm$ 0.045
$Z \to ee$	0.000 $\pm$ 0.429	0.000 $\pm$ 0.429	0.000 $\pm$ 0.429	0.000 $\pm$ 0.429
$Z \to \mu\mu$	0.000 $\pm$ 0.429	0.000 $\pm$ 0.429	0.000 $\pm$ 0.429	0.000 $\pm$ 0.429
$Z \to \tau\tau$	0.000 $\pm$ 0.429	0.000 $\pm$ 0.429	0.000 $\pm$ 0.429	0.000 $\pm$ 0.429
W+jets	0.000 $\pm$ 1.808	0.000 $\pm$ 1.808	0.000 $\pm$ 1.808	0.000 $\pm$ 1.808
WW	0.000 $\pm$ 0.019	0.000 $\pm$ 0.019	0.000 $\pm$ 0.019	0.000 $\pm$ 0.019
Vγ	0.000 $\pm$ 0.248	0.000 $\pm$ 0.248	0.000 $\pm$ 0.248	0.000 $\pm$ 0.248
$W\gamma^* \to \ell\nu ee$	0.000 $\pm$ 0.097	0.000 $\pm$ 0.097	0.000 $\pm$ 0.097	0.000 $\pm$ 0.097
$W\gamma^* \to \ell\nu\mu\mu$	0.000 $\pm$ 0.075	0.000 $\pm$ 0.075	0.000 $\pm$ 0.075	0.000 $\pm$ 0.075
$W\gamma^* \to \ell\nu\tau\tau$	0.000 $\pm$ 0.028	0.000 $\pm$ 0.028	0.000 $\pm$ 0.028	0.000 $\pm$ 0.028
WZ	0.005 $\pm$ 0.005	0.000 $\pm$ 0.003	0.000 $\pm$ 0.003	0.005 $\pm$ 0.005
ZZ	0.000 $\pm$ 0.000	0.000 $\pm$ 0.000	0.000 $\pm$ 0.000	0.000 $\pm$ 0.000
dp$W^\pm W^\pm$	0.000 $\pm$ 0.004	0.000 $\pm$ 0.004	0.000 $\pm$ 0.004	0.000 $\pm$ 0.004
sp$W^- W^-$	0.000 $\pm$ 0.001	0.000 $\pm$ 0.001	0.000 $\pm$ 0.001	0.000 $\pm$ 0.001
sp$W^+ W^+$	0.000 $\pm$ 0.006	0.000 $\pm$ 0.006	0.000 $\pm$ 0.006	0.000 $\pm$ 0.006
$t\bar{t}\gamma$	0.000 $\pm$ 0.059	0.000 $\pm$ 0.059	0.000 $\pm$ 0.059	0.000 $\pm$ 0.059
$t\bar{t}W$	0.028 $\pm$ 0.006	0.041 $\pm$ 0.006	0.077 $\pm$ 0.009	0.146 $\pm$ 0.012
$t\bar{t}Z$	0.003 $\pm$ 0.001	0.009 $\pm$ 0.003	0.009 $\pm$ 0.002	0.020 $\pm$ 0.004
$WW\gamma$	0.000 $\pm$ 0.015	0.000 $\pm$ 0.015	0.000 $\pm$ 0.015	0.000 $\pm$ 0.015
WWW	0.000 $\pm$ 0.000	0.000 $\pm$ 0.000	0.000 $\pm$ 0.000	0.000 $\pm$ 0.000
WWZ	0.000 $\pm$ 0.000	0.000 $\pm$ 0.000	0.000 $\pm$ 0.000	0.000 $\pm$ 0.000
WZZ	0.000 $\pm$ 0.000	0.000 $\pm$ 0.000	0.000 $\pm$ 0.000	0.000 $\pm$ 0.000
ZZZ	0.000 $\pm$ 0.000	0.000 $\pm$ 0.000	0.000 $\pm$ 0.000	0.000 $\pm$ 0.000
Total MC	0.079 $\pm$ 0.025	0.049 $\pm$ 0.007	0.135 $\pm$ 0.030	0.263 $\pm$ 0.039
LM6	0.000 $\pm$ 0.000	0.000 $\pm$ 0.000	0.000 $\pm$ 0.000	0.000 $\pm$ 0.000
SF	0.00 $\pm$ 0.58	0.00 $\pm$ 0.37	0.18 $\pm$ 0.55	0.18 $\pm$ 0.55
DF	0.00 $\pm$ 0.14	0.00 $\pm$ 0.10	0.00 $\pm$ 0.16	0.00 $\pm$ 0.16
SF + DF	0.00 $\pm$ 0.50 $\pm$ 0.00	0.00 $\pm$ 0.31 $\pm$ 0.00	0.18 $\pm$ 0.45 $\pm$ 0.09	0.18 $\pm$ 0.45 $\pm$ 0.09
Charge Flips	0.009 $\pm$ 0.004 $\pm$ 0.002	- $\pm$ -	0.010 $\pm$ 0.004 $\pm$ 0.002	0.019 $\pm$ 0.006 $\pm$ 0.004
MC Pred	0.036 $\pm$ 0.008 $\pm$ 0.018	0.049 $\pm$ 0.007 $\pm$ 0.025	0.086 $\pm$ 0.009 $\pm$ 0.043	0.171 $\pm$ 0.014 $\pm$ 0.086
Total Pred	0.045 $\pm$ 0.501 $\pm$ 0.018	0.049 $\pm$ 0.315 $\pm$ 0.025	0.272 $\pm$ 0.447 $\pm$ 0.098	0.366 $\pm$ 0.447 $\pm$ 0.123
data	1	0	1	2

Table 18: Observed event yields in the exclusive low-H_T high-$\not{E}_T$ region (200 $< H_T <$ 320 GeV, $\not{E}_T>$ 120 GeV) compared to expectations from simulation alone, and from the data-driven methods. The upper part of the table is based on simulation only and is used only as a reference. The lower part is the main result of the analysis. The SF (DF) contributions are for events with one (two) fake leptons. The *MC Pred* contribution includes contributions from genuine same-sign lepton pairs (a sum of the rows from $V\gamma$ down to ZZZ). Entries with zero contributing events are reported with an uncertainty corresponding to one event. This uncertainty is not added to the total MC contribution. Systematic uncertainties (the second uncertainty if present) are displayed only for the final combined type of background, no systematic uncertainty is added for estimates with zero entries. Systematic uncertainties are 100% correlated among the channels.

Source	ee	$\mu\mu$	eμ	all
$t\bar{t} \to \ell\ell X$	0.151 $\pm$ 0.056	0.000 $\pm$ 0.199	0.081 $\pm$ 0.199	0.232 $\pm$ 0.066
$t\bar{t}$ other	0.000 $\pm$ 0.199	0.000 $\pm$ 0.199	0.000 $\pm$ 0.199	0.000 $\pm$ 0.199
$t\bar{t} \to \ell(b \to \ell)X$	0.016 $\pm$ 0.199	0.014 $\pm$ 0.199	0.025 $\pm$ 0.199	0.055 $\pm$ 0.199
$t\bar{t} \to \ell(\not{b} \to \ell)X$	0.135 $\pm$ 0.047	0.000 $\pm$ 0.199	0.149 $\pm$ 0.054	0.284 $\pm$ 0.072
t, s-channel	0.000 $\pm$ 0.057	0.000 $\pm$ 0.057	0.000 $\pm$ 0.057	0.000 $\pm$ 0.057
t, t-channel	0.000 $\pm$ 0.055	0.000 $\pm$ 0.055	0.000 $\pm$ 0.055	0.000 $\pm$ 0.055
tW	0.000 $\pm$ 0.045	0.000 $\pm$ 0.045	0.016 $\pm$ 0.045	0.016 $\pm$ 0.045
$Z \to ee$	0.000 $\pm$ 0.429	0.000 $\pm$ 0.429	0.000 $\pm$ 0.429	0.000 $\pm$ 0.429
$Z \to \mu\mu$	0.000 $\pm$ 0.429	0.000 $\pm$ 0.429	0.000 $\pm$ 0.429	0.000 $\pm$ 0.429
$Z \to \tau\tau$	0.000 $\pm$ 0.429	0.000 $\pm$ 0.429	0.000 $\pm$ 0.429	0.000 $\pm$ 0.429
W+jets	0.000 $\pm$ 1.808	0.000 $\pm$ 1.808	0.000 $\pm$ 1.808	0.000 $\pm$ 1.808
WW	0.000 $\pm$ 0.019	0.000 $\pm$ 0.019	0.000 $\pm$ 0.019	0.000 $\pm$ 0.019
Vγ	0.000 $\pm$ 0.248	0.000 $\pm$ 0.248	0.000 $\pm$ 0.248	0.000 $\pm$ 0.248
$W\gamma^* \to \ell\nu ee$	0.000 $\pm$ 0.097	0.000 $\pm$ 0.097	0.000 $\pm$ 0.097	0.000 $\pm$ 0.097
$W\gamma^* \to \ell\nu\mu\mu$	0.000 $\pm$ 0.075	0.000 $\pm$ 0.075	0.000 $\pm$ 0.075	0.000 $\pm$ 0.075
$W\gamma^* \to \ell\nu\tau\tau$	0.000 $\pm$ 0.028	0.000 $\pm$ 0.028	0.000 $\pm$ 0.028	0.000 $\pm$ 0.028
WZ	0.005 $\pm$ 0.005	0.012 $\pm$ 0.007	0.004 $\pm$ 0.004	0.020 $\pm$ 0.009
ZZ	0.000 $\pm$ 0.000	0.000 $\pm$ 0.000	0.000 $\pm$ 0.000	0.000 $\pm$ 0.000
dp$W^{\pm}W^{\pm}$	0.000 $\pm$ 0.004	0.000 $\pm$ 0.004	0.000 $\pm$ 0.004	0.000 $\pm$ 0.004
sp$W^{-}W^{-}$	0.000 $\pm$ 0.001	0.000 $\pm$ 0.001	0.001 $\pm$ 0.001	0.001 $\pm$ 0.001
sp$W^{+}W^{+}$	0.000 $\pm$ 0.006	0.000 $\pm$ 0.006	0.000 $\pm$ 0.006	0.000 $\pm$ 0.006
$t\bar{t}\gamma$	0.000 $\pm$ 0.059	0.000 $\pm$ 0.059	0.000 $\pm$ 0.059	0.000 $\pm$ 0.059
$t\bar{t}W$	0.147 $\pm$ 0.013	0.175 $\pm$ 0.014	0.277 $\pm$ 0.017	0.599 $\pm$ 0.026
$t\bar{t}Z$	0.027 $\pm$ 0.004	0.035 $\pm$ 0.005	0.059 $\pm$ 0.006	0.120 $\pm$ 0.009
$WW\gamma$	0.000 $\pm$ 0.015	0.000 $\pm$ 0.015	0.000 $\pm$ 0.015	0.000 $\pm$ 0.015
WWW	0.000 $\pm$ 0.000	0.000 $\pm$ 0.000	0.000 $\pm$ 0.000	0.000 $\pm$ 0.000
WWZ	0.000 $\pm$ 0.000	0.000 $\pm$ 0.000	0.001 $\pm$ 0.001	0.001 $\pm$ 0.001
WZZ	0.000 $\pm$ 0.000	0.000 $\pm$ 0.000	0.000 $\pm$ 0.000	0.000 $\pm$ 0.000
ZZZ	0.000 $\pm$ 0.000	0.000 $\pm$ 0.000	0.000 $\pm$ 0.000	0.000 $\pm$ 0.000
Total MC	0.480 $\pm$ 0.076	0.236 $\pm$ 0.021	0.614 $\pm$ 0.074	1.329 $\pm$ 0.108
LM6	0.000 $\pm$ 0.000	0.000 $\pm$ 0.000	0.000 $\pm$ 0.000	0.000 $\pm$ 0.000
SF	0.24 $\pm$ 0.55	0.00 $\pm$ 0.37	0.27 $\pm$ 0.59	0.51 $\pm$ 0.75
DF	0.00 $\pm$ 0.14	0.00 $\pm$ 0.10	0.00 $\pm$ 0.16	0.00 $\pm$ 0.16
SF + DF	0.24 $\pm$ 0.47 $\pm$ 0.12	0.00 $\pm$ 0.31 $\pm$ 0.00	0.27 $\pm$ 0.49 $\pm$ 0.14	0.51 $\pm$ 0.68 $\pm$ 0.25
Charge Flips	0.065 $\pm$ 0.012 $\pm$ 0.013	- $\pm$ -	0.079 $\pm$ 0.011 $\pm$ 0.016	0.144 $\pm$ 0.017 $\pm$ 0.029
MC Pred	0.178 $\pm$ 0.014 $\pm$ 0.089	0.222 $\pm$ 0.016 $\pm$ 0.111	0.344 $\pm$ 0.019 $\pm$ 0.172	0.744 $\pm$ 0.029 $\pm$ 0.372
Total Pred	0.479 $\pm$ 0.473 $\pm$ 0.148	0.222 $\pm$ 0.315 $\pm$ 0.111	0.694 $\pm$ 0.495 $\pm$ 0.219	1.394 $\pm$ 0.685 $\pm$ 0.451
data	0	0	1	1

Table 19: Observed event yields in the exclusive low-H_T low-$\not{E}_T$ region ($200 < H_T < 320$ GeV, $50 < \not{E}_T < 120$ GeV) compared to expectations from simulation alone, and from the data-driven methods. The upper part of the table is based on simulation only and is used only as a reference. The lower part is the main result of the analysis. The SF (DF) contributions are for events with one (two) fake leptons. The *MC Pred* contribution includes contributions from genuine same-sign lepton pairs (a sum of the rows from $V\gamma$ down to ZZZ). Entries with zero contributing events are reported with an uncertainty corresponding to one event. This uncertainty is not added to the total MC contribution. Systematic uncertainties (the second uncertainty if present) are displayed only for the final combined type of background, no systematic uncertainty is added for estimates with zero entries. Systematic uncertainties are 100% correlated among the channels.

Source	ee	$\mu\mu$	eμ	all
$t\bar{t} \to \ell\ell X$	0.067 $\pm$ 0.199	0.000 $\pm$ 0.199	0.061 $\pm$ 0.199	0.129 $\pm$ 0.047
$t\bar{t}$ other	0.000 $\pm$ 0.199	0.000 $\pm$ 0.199	0.000 $\pm$ 0.199	0.000 $\pm$ 0.199
$t\bar{t} \to \ell(b \to \ell)X$	0.025 $\pm$ 0.199	0.020 $\pm$ 0.199	0.019 $\pm$ 0.199	0.065 $\pm$ 0.199
$t\bar{t} \to \ell(\not{b} \to \ell)X$	0.076 $\pm$ 0.199	0.016 $\pm$ 0.199	0.138 $\pm$ 0.053	0.230 $\pm$ 0.066
t, s-channel	0.000 $\pm$ 0.057	0.000 $\pm$ 0.057	0.000 $\pm$ 0.057	0.000 $\pm$ 0.057
t, t-channel	0.000 $\pm$ 0.055	0.000 $\pm$ 0.055	0.000 $\pm$ 0.055	0.000 $\pm$ 0.055
tW	0.000 $\pm$ 0.045	0.000 $\pm$ 0.045	0.000 $\pm$ 0.045	0.000 $\pm$ 0.045
$Z \to ee$	0.000 $\pm$ 0.429	0.000 $\pm$ 0.429	0.000 $\pm$ 0.429	0.000 $\pm$ 0.429
$Z \to \mu\mu$	0.000 $\pm$ 0.429	0.000 $\pm$ 0.429	0.000 $\pm$ 0.429	0.000 $\pm$ 0.429
$Z \to \tau\tau$	0.000 $\pm$ 0.429	0.000 $\pm$ 0.429	0.000 $\pm$ 0.429	0.000 $\pm$ 0.429
W+jets	0.000 $\pm$ 1.808	0.000 $\pm$ 1.808	0.000 $\pm$ 1.808	0.000 $\pm$ 1.808
WW	0.000 $\pm$ 0.019	0.000 $\pm$ 0.019	0.000 $\pm$ 0.019	0.000 $\pm$ 0.019
Vγ	0.000 $\pm$ 0.248	0.000 $\pm$ 0.248	0.000 $\pm$ 0.248	0.000 $\pm$ 0.248
$W\gamma^* \to \ell\nu ee$	0.000 $\pm$ 0.097	0.000 $\pm$ 0.097	0.000 $\pm$ 0.097	0.000 $\pm$ 0.097
$W\gamma^* \to \ell\nu\mu\mu$	0.000 $\pm$ 0.075	0.000 $\pm$ 0.075	0.000 $\pm$ 0.075	0.000 $\pm$ 0.075
$W\gamma^* \to \ell\nu\tau\tau$	0.000 $\pm$ 0.028	0.000 $\pm$ 0.028	0.000 $\pm$ 0.028	0.000 $\pm$ 0.028
WZ	0.005 $\pm$ 0.005	0.000 $\pm$ 0.003	0.006 $\pm$ 0.004	0.011 $\pm$ 0.006
ZZ	0.000 $\pm$ 0.000	0.000 $\pm$ 0.000	0.000 $\pm$ 0.000	0.000 $\pm$ 0.000
dp$W^{\pm}W^{\pm}$	0.000 $\pm$ 0.004	0.000 $\pm$ 0.004	0.000 $\pm$ 0.004	0.000 $\pm$ 0.004
sp$W^{-}W^{-}$	0.000 $\pm$ 0.001	0.000 $\pm$ 0.001	0.000 $\pm$ 0.001	0.000 $\pm$ 0.001
sp$W^{+}W^{+}$	0.000 $\pm$ 0.006	0.000 $\pm$ 0.006	0.000 $\pm$ 0.006	0.000 $\pm$ 0.006
$t\bar{t}\gamma$	0.000 $\pm$ 0.059	0.000 $\pm$ 0.059	0.000 $\pm$ 0.059	0.000 $\pm$ 0.059
$t\bar{t}W$	0.131 $\pm$ 0.012	0.134 $\pm$ 0.012	0.247 $\pm$ 0.016	0.512 $\pm$ 0.024
$t\bar{t}Z$	0.024 $\pm$ 0.004	0.041 $\pm$ 0.005	0.062 $\pm$ 0.006	0.127 $\pm$ 0.009
$WW\gamma$	0.000 $\pm$ 0.015	0.000 $\pm$ 0.015	0.000 $\pm$ 0.015	0.000 $\pm$ 0.015
WWW	0.000 $\pm$ 0.000	0.000 $\pm$ 0.000	0.001 $\pm$ 0.000	0.001 $\pm$ 0.001
WWZ	0.000 $\pm$ 0.000	0.000 $\pm$ 0.000	0.000 $\pm$ 0.000	0.000 $\pm$ 0.000
WZZ	0.000 $\pm$ 0.000	0.000 $\pm$ 0.000	0.000 $\pm$ 0.000	0.000 $\pm$ 0.000
ZZZ	0.000 $\pm$ 0.000	0.000 $\pm$ 0.000	0.000 $\pm$ 0.000	0.000 $\pm$ 0.000
Total MC	0.329 $\pm$ 0.055	0.211 $\pm$ 0.026	0.535 $\pm$ 0.069	1.075 $\pm$ 0.092
LM6	0.000 $\pm$ 0.000	0.000 $\pm$ 0.000	0.000 $\pm$ 0.000	0.000 $\pm$ 0.000
SF	0.27 $\pm$ 0.54	0.00 $\pm$ 0.37	0.39 $\pm$ 0.57	0.66 $\pm$ 0.72
DF	0.00 $\pm$ 0.14	0.00 $\pm$ 0.10	0.00 $\pm$ 0.16	0.00 $\pm$ 0.16
SF + DF	0.27 $\pm$ 0.45 $\pm$ 0.14	0.00 $\pm$ 0.31 $\pm$ 0.00	0.39 $\pm$ 0.47 $\pm$ 0.19	0.66 $\pm$ 0.65 $\pm$ 0.33
Charge Flips	0.035 $\pm$ 0.009 $\pm$ 0.007	- $\pm$ -	0.057 $\pm$ 0.011 $\pm$ 0.011	0.092 $\pm$ 0.014 $\pm$ 0.018
MC Pred	0.160 $\pm$ 0.014 $\pm$ 0.080	0.175 $\pm$ 0.013 $\pm$ 0.088	0.316 $\pm$ 0.018 $\pm$ 0.158	0.651 $\pm$ 0.026 $\pm$ 0.326
Total Pred	0.468 $\pm$ 0.453 $\pm$ 0.159	0.175 $\pm$ 0.315 $\pm$ 0.088	0.759 $\pm$ 0.470 $\pm$ 0.250	1.402 $\pm$ 0.653 $\pm$ 0.464
data	1	1	0	2

Table 20: Observed event yields in the exclusive high-H_T low-$\not{E}_T$ region ($H_T > 320$ GeV, $50 < \not{E}_T < 120$ GeV) compared to expectations from simulation alone, and from the data-driven methods. The upper part of the table is based on simulation only and is used only as a reference. The lower part is the main result of the analysis. The SF (DF) contributions are for events with one (two) fake leptons. The *MC Pred* contribution includes contributions from genuine same-sign lepton pairs (a sum of the rows from $V\gamma$ down to ZZZ). Entries with zero contributing events are reported with an uncertainty corresponding to one event. This uncertainty is not added to the total MC contribution. Systematic uncertainties (the second uncertainty if present) are displayed only for the final combined type of background, no systematic uncertainty is added for estimates with zero entries. Systematic uncertainties are 100% correlated among the channels.